ANALYSIS OF EPR SPECTRUM USING GRADIENT PROJECTION AND GAUSS NEWTON METHODS

BY

Nuttaka Tantragul

MASTER OF ELECTRICAL ENGINEERING

KING MONGUT INSTITUTE OF TECHNOLOGY

LADKRABANG CAMPUS.

1979

ANALYSIS OF EPR SPECTRUM USING GRADIENT PROJECTION AND GAUSS NEWTON METHODS

by

Nuttaka Tantragul

A Thesis Submitted to the Graduate
Department of Electrical Engineering
in Partial Fulfillment of the
Requirements for the Degree of

MASTER OF ELECTRICAL ENGINEERING

Major Subject : Electrical Engineering

Approved:

Dr. Daniel Phillip Breen , Thesis Adviser

KING MONGUT INSTITUTE OF TECHNOLOGY
LADKRABANG CAMPUS
1979

CONTENTS

LIST OF FIGURE

LIST OF TABLES

ACKNOWLEDGEMENT

The author wishes to thank Dr. Daniel Phillip Breen for guidance and encouragement received under his supervision and his kindness in grammatical correction.

Thanks are also made to Flying Officer Jirachai Kromvetch for the contribution of his drawing skill.

Special thanks are extended to Air Vice Marshall Dr. Bisuddi Riddhagni,director of the Systems Research and Computing Center Institute of Research and Developement,Royal Thai Air Force,and Flying Officer Wiroj Homsup for their advice and assistance.

ABSTRACT

Calculations have been made to analyse an experimental electron paramagnetic resonance spectrum influenced by Jahn-Teller Effect. The spectrum is of a Cu^{2+} ion in highly symmetric surroundings. In such systems the low temperature spectrum shows a discrete hyperfine structure corresponding to each of three separate directions of distortion. At high temperature the Jahn-Teller Effect leads to an averaging of these spectra and the resulting spectrum observed consists of four overlapping lines. The theory of the process predicts the line shape of the individual lines as well as parameters that vary within the components of the composite spectrum.

A theoretical expression has been fitted to the experimental spectrum using a least squares method. Improved fitting resulted from use of the Gauss-Newton method. However it was found that the method of analysis best suited to the constraints of the physical problem is that of Gradient Projection. The results obtained using this method are presented and comparision made with parameters predicted by current physical theory. The computing program is written for H.P.45 computer (HEWLETT PACKARD 9845A) in the BASIC language.

PART 1
INTRODUCTION

In the year 1937,a very general phenomenon, which has since become known as the Jahn-Teller Effect after its discoverer,was predicted (4) . In brief, Jahn and Teller showed that a crystal whose symmetry is such that the energy levels of an electronic complex are degenerate will undergo a spontaneous distortion to remove this degeneracy. Such behavior is exemplified by a Cu^{2+} ion in an octahedron of water molecules. The ground electronic state is an orbital doublet, separated from an upper triplet by the electric field of the surrounding ions. By group theoretical arguments Jahn and Teller demonstrated that for every such degeneracy there exists at least one distortion of the symmetrically placed surroundings which will split the degenerate levels. As the center of gravity of the energy levels is unchanged it follows that some levels will be below the unperturbed state, leading to an overall lowering of the electronic energy in the crystal. The distortion of the lattice involves an increase in elastic energy. A balance between these counteracting forces will lead to a minimum totol energy for a finite distortion. However , recent theory has indicated that the Jahn-Teller Effect gives rise to a set of vibrational energy levels which one would expect to become populated as the temperature rises. Some of these levels involved, the spectrum of the copper ion has been traced over a range of temperature about the transition. The influence of vibronic transitions can be deduced from variations in the spectral line shape and widths. Early analysis indicated agreement with other methods previously used to study vibronic transitions, and extended knowledge of their temperature dependence.In this thesis, we use a computer to analyse an experimental spectrum of Cu^{2+} in lanthanum magnesium nitrate. The hyperfine structure of copper is of interest as being the first to be discovered in the solid state by the method of electron paramagnetic resonance and the electron magnetic resonance spectrum of the cupric ion is also noteworthy as the first example in which an effect due to the nuclear electric quadrupole interaction was observed. An experimental spectrum were collected from an experiment performed by Dr. Daniel P. Breen. This thesis is the extension of Dr. Breen's work. This thesis uses a computer to analyse the spectrum by

Gauss-Newton and Gradient Projection methods. A function is constructed by squaring the difference between a theoretical expression for the electron paramagnetic resonance spectrum and experimental values. This function is then minimized my computer computation.

Gauss-Newton algorithm(1) is the method used to minimize a function of several variables. We expand the function by Tayler expansion. The function is a minimum when all its derivatives with respect to each variable are zero.

Gradient Projection(2) is an alternative approach to optimization introduced by J.B.Rosen. It is an iterative numerical produre for finding an extremum of a function of several variables that are required to satisfy various linear constraining relations. We use Gradient Projection as applied to least square problems that have linear constraints. One advantage of Gradient Projection method over the Gauss-Newton method is its flexibility of initial condition.

PART 2

THEORETICAL BACKGROUND

2.1 Electron para magnetic resonance.

Consider a single paramagnetic ion Cu^{2+} ,of moment $\vec{m}$, in a magnetic field $\vec{H}$,(in this thesis use lantanium magnesium double nitrate) ,its energy is given by $-\vec{m}.\vec{H}$. Now if the direction of $\vec{H}$ is taken as the z direction and $\vec{m}$ is written in term of the electron spin $\vec{S}$ which gives rise to magnetism $\vec{m} = g\beta\vec{S}$ where g is a constant and β is the Bohr magneton , then energy $\vec{E}$ is

$$\begin{aligned} \vec{E} &= -g\beta\vec{S}.\vec{H} \\ &= -g\beta S_z H_z \end{aligned} \qquad \text{.....(2.1.1)}$$

For Cu^{2+} electron spin = 1/2 this gives two states to $S_z = \pm 1/2$ which can be shown as

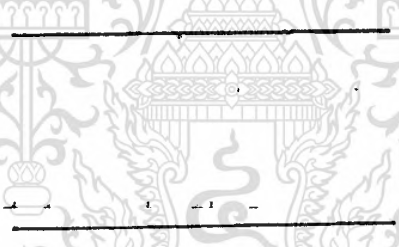

Fig 2.1.1 Energy state corresponding to $S_z = \pm 1/2$

and transition can be induced between the states by radiation of frequency

$$\begin{aligned} \Delta E &= E_2 - E_1 \\ &= g\beta H \\ &= h\nu \end{aligned} \qquad \text{.....(2.1.2)}$$

But the nucleus of Cu^{2+} has spin too. It also has a magnetic moment which interacts with that of the electron spin to give energy states shown for this case S=1/2 , I=3/2 , the energy level of equation (2.1.1)

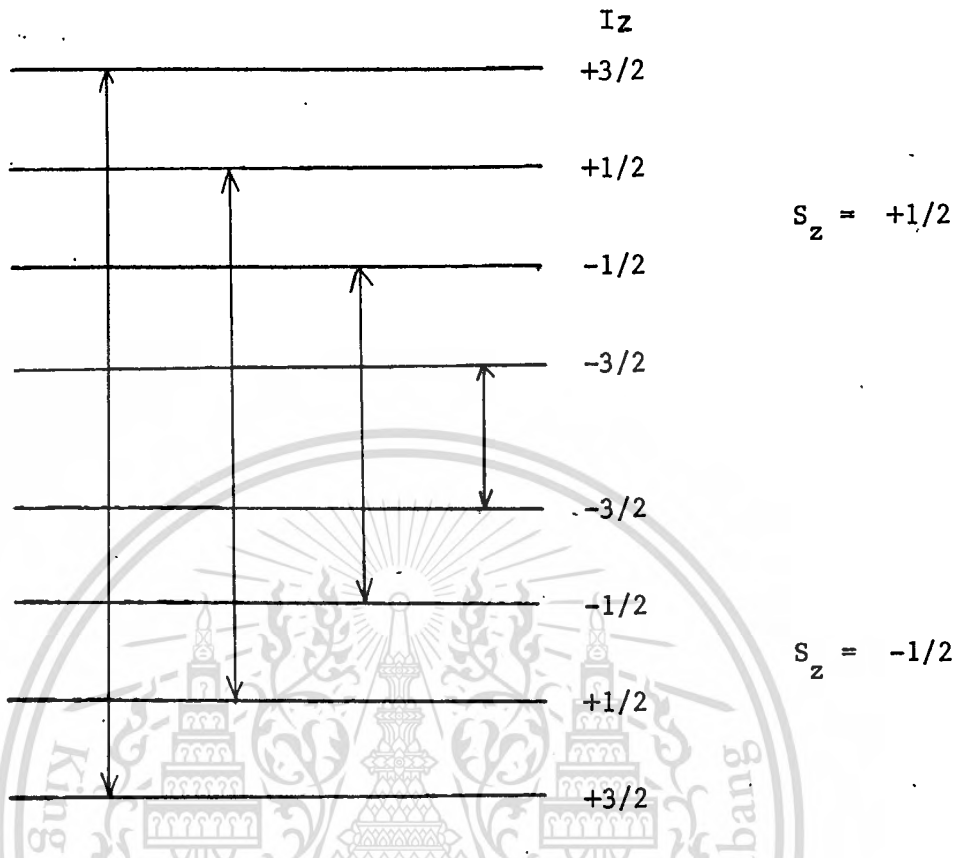

Fig. 2.1.2 Energy states corresponding to $S_z = 1/2$ and $I_z = 3/2$

We should be able to detect the presence of such a set of energy levels by some form of spectral absorbtion. The transitions between levels must satisfy the conservation of energy, the interaction must be time dependent and of such an angular frequency ω that

$$\hbar\omega = \Delta E \qquad .....(2.1.3)$$

ΔE is the energy difference between the initial and final nuclear Zeeman energies.

The coupling most commonly used to produce magnetic resonances, is an alternating magnetic field applied perpendicular to the static field. For values of the magnetic field easily available in the laboratory ($\sim$ 0.3 to 0.4 tesla) the frequency ω falls in the microwave range and the technique of studying energy separation by absorbtion of microwave power is called electron paramagnetic resonance (EPR) . For example Fig.2.1.2 shows that a total of four lines are observed between the states $S_z = +1/2$, $S_z = -1/2$ (nuclear transitions $\Delta I_z = 0$ only are allowed by the quantum mechanical selection rules). This spectrum of four lines is the subject of study in the present thesis.

The experiment was carried out on Cu^{2+} in lanthanum magnesium double nitrate. The observed spectral line is described by a Lorentzian shape.

$$F(H) = \frac{2A}{a} \frac{a}{(a^2+(H-\Delta H)^2)^2} \quad \ldots(2.1.4)$$

F(H) = normalized line shape function.

a = the line width.

H = is considered as the variable.

a is determined by quantum process involving the transition probability or life time of the electron in the higher energy state.

In general the shape of EPR lines has two forms known as inhomogeneous and homogeneous.

2.1.1. Inhomogeneous lines.

The magnetic fields due to other magnetic moments in the solid cause small shifts in the energy levels which vary in a random way fromsite to site. The spectral line observed may then be a sum of Lorentzian shaped lines distributed in a random manner about a central position. The resulting overall line shape is called Gaussian and has the form,

$$F(H) = \frac{1}{(2\P<H_i^2>)^{\frac{1}{2}}} \exp\frac{-(H-H_0)^2}{2<H_i>^2} \quad \ldots(2.1.5)$$

where H_0 = the centre of the resonance line being scanned in field.

$<H_i>$ = described the distribution of random fields inside the solid.

2.1.2. Homogeneous lines.

Interaction of the magnetic ions with the phonon spectrum of the solid causes a change in the line width of the individual spectral lines which is temperature dependent. At high temperature this can cause the Lorentzian line width to be greater than that caused by the effect of randomfield and the overall line shape observed becomes Lorentzian shape.

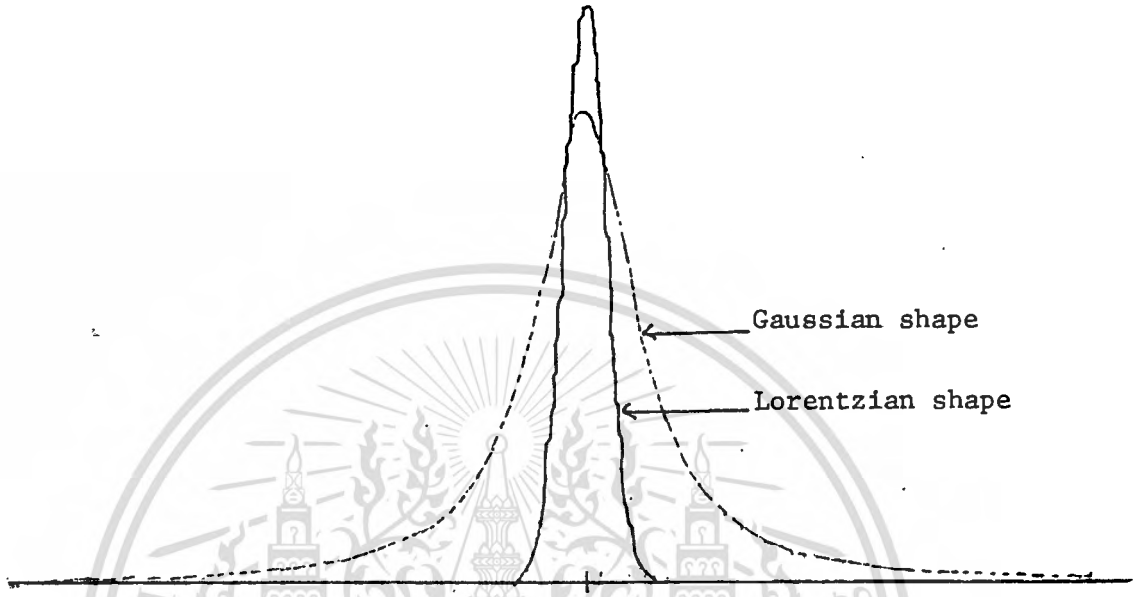

Fig. 2.1.3. Gaussian and Lorentzian shapes.

2.2. Spin Hamiltonian

The outline of EPR given in section 2.1 depicted a very simple energy level system due to electron and nuclear spin only. In fact account must also be taken of magnetism due to orbital momentum L.

The method followed is to write down the Hamiltonian including all energy interaction of the ion . Energy levels are then found by soling the Schrödinger equation

$$H\Psi = E\Psi \qquad .....(2.2.1)$$

A simple form of the Hamiltonian including the effect of angular momentum would take the form

$$H = \beta\vec{H}.(\vec{L}+2\vec{S}) + \lambda\vec{L}.\vec{S} + \gamma\vec{I}.\vec{S} \qquad .....(2.2.2)$$

where the first term expresses interaction with the external magnetic field $\vec{H}$, the second term is an orbital spin interaction and the last

term is the energy of interaction between electron and nuclear spins.

Calculation using the Hamiltonian from equation (2.2.2) ~~are~~ is complex. In case of strong crystal field where electron levels for different values of L are widely seperated it has been found possible to treat the ground levels in term of spin $\vec{S}$ only so that the effects of orbital angular momentum are included in the constants. The result is called the Spin Hamiltonian and values of the energy levels can be derived by solving the eigenvalue equation (2.2.1) by diagonalizing the matrix of H.

The Spin Hamiltonian corresponding to equation (2.2.2) has the form

$$H = \beta (g_x H_x S_x + g_y H_y S_y + g_z H_z S_z) + A_x S_x I_x + A_y S_y I_y + A_z S_z I_z \quad \ldots(2.2.3)$$

In the case where $H = H_z$ and $A_y = A_x$ (axial symmetry)

$$H = g_{//}\beta H S_z + A_{//} S_z I_z + A_{\perp}(S_x I_x + S_y I_y) \quad \ldots(2.2.4)$$

A more complete Spin Hamiltonian including the effects of nuclear quadrupole moment and interaction between the magnetic field and the nuclear spin is given by

$$H = g_{//}\beta H_z S_z + A_{//} S_z I_z + A_{\perp}(S_x I_x + S_y I_y) + P_{//}(I_z^2 - 1/3\, I(I+1)) + g_n \beta_n H_z I_z \quad \ldots(2.2.5)$$

The vales of the constants are derived from EPR measurements [10]

2.3 Method of diagonalization.

In the results we have arbitrary units, we must change H to energy units by the diagonolization method.

From spin Hamiltonian

$$H = g\beta \vec{H}.\vec{S} + A\, \vec{I}.\vec{S}$$

$$= 9300\times10^{6}\, S_z + (26.55\times10^{-4}\times2.998\times10^{10}) \ldots\ldots(2.3.1)$$

$$(S_x I_x + S_y I_y + S_z I_z)$$

For S=1/2

$$S_x = \frac{\hbar}{2}\begin{bmatrix} 0 & 1 \\ 1 & 0 \end{bmatrix} \qquad S_y = \frac{\hbar}{2}\begin{bmatrix} 0 & -i \\ i & 0 \end{bmatrix} \qquad S_z = \frac{\hbar}{2}\begin{bmatrix} 1 & 0 \\ 0 & -1 \end{bmatrix}$$

For I= 3/2

$$I_x = \frac{\hbar}{2}\begin{bmatrix} 0 & \sqrt{3} & 0 & 0 \\ \sqrt{3} & 0 & 2 & 0 \\ 0 & 2 & 0 & \sqrt{3} \\ 0 & 0 & \sqrt{3} & 0 \end{bmatrix} \quad I_y = \frac{\hbar}{2}\begin{bmatrix} 0 & -i\sqrt{3} & 0 & 0 \\ i\sqrt{3} & 0 & -2i & 0 \\ 0 & 2i & 0 & -i\sqrt{3} \\ 0 & 0 & i\sqrt{3} & 0 \end{bmatrix} \quad I_z = \frac{\hbar}{2}\begin{bmatrix} 3 & 0 & 0 & 0 \\ 0 & 1 & 0 & 0 \\ 0 & 0 & -1 & 0 \\ 0 & 0 & 0 & -3 \end{bmatrix}$$

$$H = 10^6 \begin{bmatrix} 4650+3/4x79.597 & 0 & 0 & 0 & 0 & 0 & 0 & 0 \\ 0 & 4650+1/4x79.597 & 0 & 0 & \sqrt{3}/2x79.597 & 0 & 0 & 0 \\ 0 & 0 & 4650-1/4x79.597 & 0 & 0 & 79.597 & 0 & 0 \\ 0 & 0 & 0 & 4650-3/4x79.597 & 0 & 0 & \sqrt{3}/2x79.597 & 0 \\ 0 & 0 & 0 & 0 & -4650-3/4x79.597 & 0 & 0 & 0 \\ \sqrt{3}/2x79.597 & 0 & 0 & 0 & -4650-1/4x79.597 & 0 & 0 & 0 \\ 0 & 79.597 & 0 & 0 & 0 & 0 & -4650+1/4x79.597 & 0 \\ 0 & 0 & \sqrt{3}/2x79.597 & 0 & 0 & 0 & 0 & -4650+3/4x79.5969 \end{bmatrix}$$

By diagonolization, we obtain

$$H = 10^9 \begin{bmatrix} 4.709698 & & & & & & & \\ & 4.669899 & & & & & & \\ & & 4.630101 & & & & & \\ & & & 4.590302 & & & & \\ & & & & -4.709698 & & & \\ & & & & & -4.669899 & & \\ & & & & & & -4.630101 & \\ & & & & & & & -4.590302 \end{bmatrix}$$

The diagonolized values correspond to energy levels in the eigenvalue equation.

$$H\Psi = E\Psi \qquad \ldots(2.3.2)$$

In this case we have 8 energy levels.

$$\Delta S_z = 1/2 \qquad \ldots(2.3.3)$$

$$\Delta I_z = 0 \qquad \ldots(2.3.4)$$

WE get 4 lines.

$$E_1 - E_5 = 9419.396\times10^6 \text{ Hz}$$
$$E_2 - E_6 = 9339.798\times10^6 \text{ Hz}$$
$$E_3 - E_7 = 9260.202\times10^6 \text{ Hz}$$
$$E_4 - E_8 = 9180.604\times10^6 \text{ Hz}$$

For diagonolization matrix

$$\begin{bmatrix} E_1 & & & & & & & \\ & E_2 & & & & & & \\ & & E_3 & & & & & \\ & & & E_4 & & & & \\ & & & & E_5 & & & \\ & & & & & E_6 & & \\ & & & & & & E_7 & \\ & & & & & & & E_8 \end{bmatrix}$$

The frequency difference between these four lines is given by

$$(E_1 - E_5) - (E_2 - E_6) = 79.598\times10^6 \text{ Hz}$$
$$(E_2 - E_6) - (E_3 - E_7) = 79.596\times10^6 \text{ Hz}$$
$$(E_3 - E_7) - (E_4 - E_8) = 79.598\times10^6 \text{ Hz}$$

This corresponds to the value of ΔH in the experimental curves which can be used to change from arbitrary units to frequency units. We can use the same conversion factor to change the linewidths "a" into frequency units as shown in table 2.3.1

From equation of line width [7]

$$a = T\{(g_{//} - g_{\perp})\beta H + (A_{//} - A_{\perp})m\}^2/h^2 \quad ..(2.3.5)$$

$$\sqrt{a} = \frac{\sqrt{T}}{h}\{(g_{//} - g_{\perp})\beta H + \frac{\sqrt{T}}{h}(A_{//} - A_{\perp})m \quad .(2.3.6)$$

We plot a againt m and use least square fit to find the best straight line and slope as shown in table 2.3.2

$$T = h\,(\text{slope}^2) / (A_{//} - A_{\perp})^2 \quad ..(2.3.7)$$

We can plot 1/ T againt T^5 in Fig 4.4.1

Table 2.3.1 Line width in frequency units.

T K	a_1(hz)	a_2(hz)	a_3(hz)	a_4(hz)
76.4	111397578.151	92487318.487	177798484.874	141602394.118
77.0	36295881.738	48213540.374	67075139.714	89491896.590
80.2	571824226.452	651071605.661	319195505.797	328885575.362
84.0	108120204.565	175647074.608	246512249.643	192236406.562
92.2	112043410.687	233687070.229	216917015.267	210840908.397
102.8	98192563.424	181717265.960	161701516.309	185911253.415
110.4	120381900.000	214665300.000	229187300.000	180381050.000
77.0	28251297.155	36175105.485	43228286.753	49702886.744

Table 2.3.2 Slope.

Temperature°K	m	a	a (Hz)	Slope(1/√Hz)
76.4°	-1.5	11.658	111397578.151	775.26± 1.234
	-0.5	9.679	92487318.487	
	0.5	18.607	177798484.874	
	1.5	14.819	141602394.118	
77.0°	-1.5	4.145	36295881.738	1155.26± 376.753
	-0.5	5.506	48213540.374	
	0.5	7.660	67075139.714	
	1.5	10.220	89491896.590	
80.2°	-1.5	14.720	169806933.333	1927.40± 0.004
	-0.5	16.760	193339959.42	
	0.5	27.670	319195505.797	
	1.5	28.510	328885575.362	
84.0°	-1.5	9.522	108120204.565	1284.81± 2.640
	-0.5	15.469	175647074.608	
	0.5	21.710	246512249.643	
	1.5	16.930	192236406.562	
92.2°	-1.5	9.220	112043410.687	1124.72± 1.664
	-0.5	19.230	233687070.229	
	0.5	17.850	216917015.267	
	1.5	17.35	210840908.397	
102.8°	-1.5	8.850	98192563.424	1041.31± 3.038
	-0.5	16.378	181717265.960	
	0.5	14.574	161701516.309	
	1.5	16.756	185911253.415	
110.4°	-1.5	8.787	120381900.000	786.367± 0.846
	-0.5	15.669	214665300.000	
	0.5	16.729	229187300.000	
	1.5	13.167	180381050.000	
77.0°	-1.5	10.254	28251297.155	1155.257± 261.470
	-0.5	13.130	36175105.485	
	0.5	15.69	43228286.753	
	1.5	18.04	49702886.744	

PART 3

THE JAHN-TELLER THEORY

3.1 Introduction

The Jahn-Teller Theorem[4] is concerned with the interaction between the energy levels of an atom and the symmetry of a crystal field. The energy levels of an atom within the electric field caused by the surrounding ions in a crystal, called the crystal field, can be solved by standard quantum mechanical methods. In fields of high symmetry it is generally found that the lower orbital levels are degenerate, while in lower symmetry fields this degeneracy is removed.

Consider an atom in a field of high symmetry such that it has degenerate orbital levels. The high symmetry arises from the fact that the crystal lattice exists in a state of minimum elastic energy. If a distortion is introduced the elastic energy increases. However the electronic degeneracy is removed and as the centre of gravity ~~of gravity~~ of perturbed states remains the same, some states must be lower in energy. The reduction in electronic energy achieved as atoms occupy these lower energy states can compensate for the increased elastic energy associated with the distortion. Jahn and Teller showed that an overall reduction in energy always occurs by distortion of a symmetric field whenever orbital states are degenerate. The only degeneracy that cannot be removed by distortion is the so-called Kramers degeneracy involving opposite electronic spin states and which can only be removed by a magnetic field.

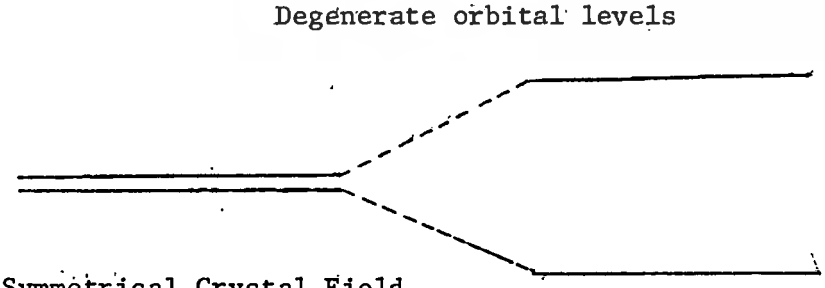

3.2 Cu^{2+} in octahedral field

The theorem can be illustrated by the case of copper ions in a crystal field of octahedral symmetry such as the subject of this thesis. Copper (atomic number 29) is the last of 3d group in the periodic table where the 29 electrons form filled shells around the nucleus with one electron in a $4s^1$ state. The Cu^{2+} ion as it occurs in ionic solids has two electron less so that its outer shell is $3d^9$. The ground state of this ion is called ^2D having a combined orbital momentum L=2 and spin S=½. Its orbital degeneracy 2L+1 is 5. A crystal field of octahedral symmetry, i.e. the electric field caused by surrounding ions located at the corners of a regular octahedral (Fig.3.2.1) splits the five fold degenerate levels into an upper triplet and a lower doublet which are labelled by the group theoretical symbols (Γ_5 and Γ_3) Fig 3.2.2. We now have the case considered by Jahn-and Teller degeneracy in a symmetric field.

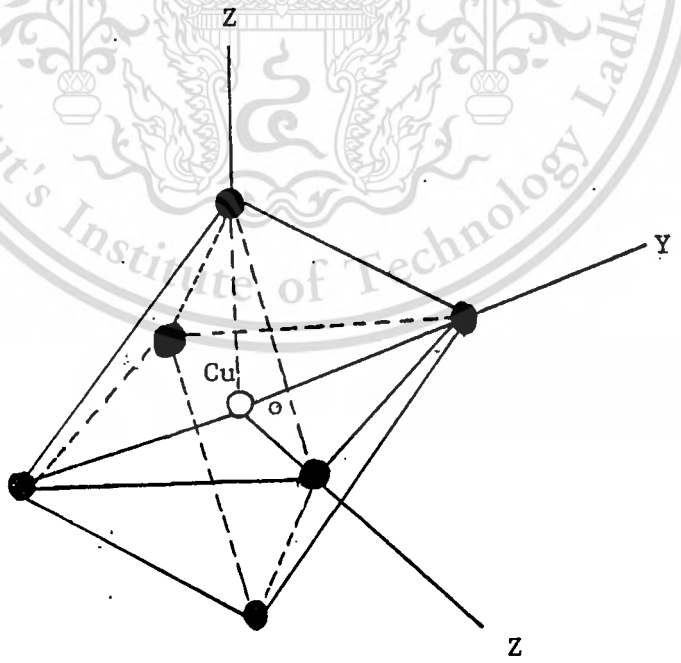

Fig.3.2.1 Cu^{2+} in octahedral field.

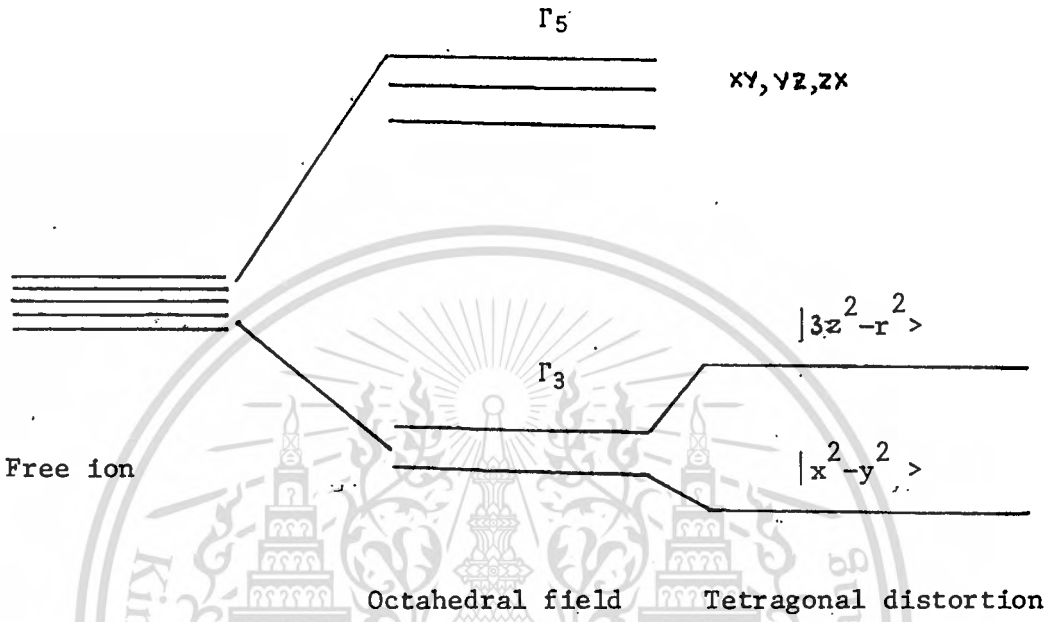

Fig.3.2.2 The degeneracy of the lowest doublet Γ_3

We expect that the degeneracy of the lowest doublet Γ_3 will be further split by distortion as shown in Fig3.2.2 where the states are identified by their orbital wave functions.

The distortion causing the splitting can be considered as combination of the normal modes of vibration of the octahedron shown in figure 3.2.3

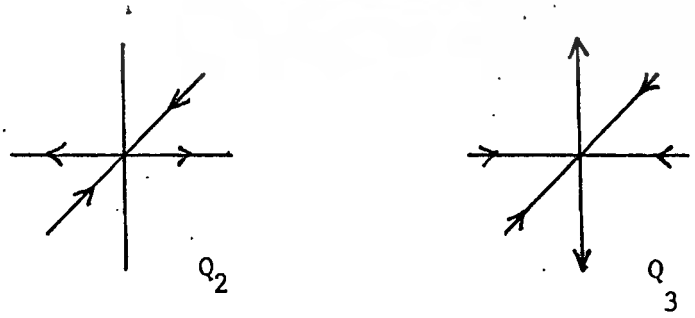

Fig.3.2.3 Normal modes of an octahedron

The change in elastic energy is proportional to the square of the displacements while the lowering in electronic energy is linear. The sum of the two effects can be expressed as a potential energy operator.

$$U = V (Q_2 U_2 + Q_3 U_3) + \frac{Mw^2}{2} (Q_2^2 + Q_3^2) I \quad ..(3.1)$$

when U_2 and U_3 are Pauli spin matrices

I is the unit matrix

M is the mass of each nucleus at an octahedron vertex

V is a constant while w is the harmonic frequency of the vibrational mode

If we introduce new variables ρ and ϕ where $Q_2 = \rho \sin\theta$ $Q_3 = \rho \cos\theta$ then the operator may be diagonolized to give the states

$$U = \pm V\rho + \frac{Mw^2 \rho^2}{2} \quad ..(3.2)$$

Differentiation gives a minimum at $\rho_o = |V| / Mw^2$ the value of minimum energy is

$$W_{JT} = | V | \rho_0 /2 \quad ..(3.3)$$

This expression is independent of ϕ while implies an infinite possible combination of values Q_2, Q_3 . However when higher order terms are included in the energy operator an extra term proportional is added and the lower energy term becauses,

$$U = -V\rho + \frac{Mw^2 \rho^2}{2} + V_3 \rho^3 \cos 3\phi \quad ..(3.4)$$

If $V_3 < 0$ this gives minimafor the discrete values of $\phi = 0, \frac{2}{3}\pi, \frac{4}{3}\pi$ The potential is shown as a set of three potential wells,Fig 3.2.4 The low energy states of the Cu^{2+} ion are the set of vibrational level which occur within these wells.

θ =	0	$\frac{2\pi}{3}$	$\frac{4\pi}{3}$
stretched axis	z	x	y

Fig 3.2.4 Potential wells in a Jahn-Teller distorted crystal field.

3.3 Electron paramagnetic resonance spectrum

The Jahn-Teller Effect does not remove spin degeneracy the application of a magnetic field causes Zeeman splitting which may be observed by the electron magnetic resonance technique. It is found experimentally that the spectrum observed depends on the temperature. At low temperatures three spectra may be identified which may be attributed to ions in the three different distortion wells of fig 3.2.4. At high temperature a single averaged spectrum is observed. Similarity to resonance lines observed in a liquid where the ions are continually undergoing reorientation has led to the interpretation that the single spectrum results from rapid transitions from one potential well to another. The transitions may be considered as due to quantum mechanical tunneling through the barrier, dependent on temperature since the barrier narrows for higher populated states. These higher states become populated by phonon induced transitions as the temperature rises.

If T is the relaxation time for transition between potential wells the width of each hyperfine line should be in freguency;

$$a = T\{(g_{//} - g_{\perp})\beta H + (A_{//} - A_{\perp})\beta m\}^2/h^2 \quad (3.3.1)$$

where $g_{//}$, $g_{\perp}$, $A_{//}$, $A_{\perp}$ are constants occuring in the spin Hamiltonium. It is seen that the line width depends on the nuclear

magnetic quantum number m. Because the seperation of the individual lines is less than the line width, the spectrum observed is produced by the overlap of the four hyperfine lines. The object of this thesis is to analyse the experimentally observed spectrum by computer into its seperate components and to compare the widths obtained with those predicted by the above theoretical formula.

In outline the procedure is as follows. From low temperature measurements the values of $g_{//}$,$g_{\perp}$,$A_{//}$ and $A_{\perp}$ are known. Assuming lorentz line shape(10) a theoretically composed combination of four lines can be generated. The line width is taken as an adjustable parameter and changed until the best match is found with the experimental spectrum. We can then compare the optimum line width with those expected from formula 3.3.1

3.4 Spin-Spin relaxation time T

In classical,terms T is a measure of the average duration in time of a wave train emitted or absorbed by an ion in the process of paramagnetic resonance.T is infinite as far as a purely inhomogeneous broading process is concerned , and it bears no simple relation to the observed line width. If we denote by $2\Delta H$ the width of the line at half the maximum intensity.

From equation (2.1.2)

$$h\Delta\nu = g(\Delta H) \qquad ....(3.4.1)$$

which we can relate to a parameter

$$T = 1/(2\P\Delta\nu) \qquad ....(3.4.2)$$

At the temperature rises,excited vibrational states become occupied which should have different magnetic resonance spectra because of their much larger splitting due to tunnelling. The rise in temperature, however, also results in a rapid increase in the rate at which transitions between the various vibronic levels are induced by the phonon spectrum. If the relaxation rate is fast compared with the frequency difference between resonance lines from the different states, these lines disappear and are replaced by a single line at the average

frequency. It is probable that such motional narrowing is responsible for the single isotropic line observed at high temperature. It means that the resonance lines from the different levels will be replaced by a single line with a g-value equal to the mean of all the g-values. The width of this averaged line should be approximately equal to

$$T \{ (g_{//} - g_{\perp}) \beta H/h \}^2$$

The lifetime T can arise from many physical causes. It has long been observed for example that the line shape for ions in a liquid is lorentzian and the linewidth is interpreted as due to a tumbling of the ions in the liquid. The changes in strain direction associated with a dynamic Jahn-Teller Effect creates a similar situation and the linewidth of the spectral lines is expected to be proportional to

$$T\{ (g_{//} - g_{\perp})\beta H + (A_{//} - A_{\perp}) m \}^2 /h^2$$

where T is a relaxation time between different orientations $g_{//}$, $g_{\perp}$ and $A_{//}$, $A_{\perp}$ are values of the electron spin-field, and electron spin - nuclear spin interaction, parallel to and perpendicular to the direction of magnetic field $\vec{H}$. It is seen that the linewidth is proportional to the nuclear magnetic quantum number m, so each of the four lines will have a different width.

PART 4

METHOD OF ANALYSIS AND RESULTS

We wish to analyse the observed spectrum to verify this theoritical expression by method of Gauss-Newton method and Gradient Project method. Gradient Project and Gauss-Newton Algorithm are used to minimize to objective least square function. The computing program is written for H.P. 45 (HEWLETT PACKARD 9845A) computer in the BASIC language.

4.1. Gauss-Newton Method

This method is used to minimize a function of several variables , nonlinear regression equation $\hat{y} = F(x_1, x_2, \ldots, x_k, \hat{A}_1, \hat{A}_2, \ldots, \hat{A}_M)$ utilizing N data points for y_i and x_k , $i=1,2,\ldots,N$; $k=1,2,\ldots,K$. The procedure is based on a linearization of the proposed model a least squares objective function is utilized. The method has proved effective where good starting estimates of the unknown coefficients are available. The algorithm process as follows;

4.1.1 The model is linearized by expanding $\hat{y}_i$ in a Tayler Series about current trial values for the coefficients and retaining the linear term only,

$$\hat{y}_i = \hat{y}_i^* + \left[\frac{\partial \hat{y}_i}{\partial \hat{A}_1}\right]^* \Delta\hat{A}_i + \left[\frac{\partial \hat{y}_i}{\partial \hat{A}_2}\right]^* \Delta\hat{A}_2 + \ldots\ldots\ldots + \left[\frac{\partial \hat{y}_i}{\partial \hat{A}_m}\right]^* \Delta\hat{A}_m \quad \ldots(4.1.1)$$

where $\Delta\hat{A}_j = \left[\hat{A}_j - \hat{A}_j^*\right]$ $\qquad j=1,2,\ldots\ldots,M$

The asterisk designates quantities evaluated at the initial trial values.

4.1.2 A least squares objective function is formulated

$$\text{Minimize} \quad S = \sum_{i=1}^{N} (y_i - \hat{y}_i)^2 \qquad \ldots(4.1.2)$$

4.1.3 The lineared model is substituted into the objective function and the " normal equations " formed by setting the partial derivatives of the objective function with respect to each coefficient equal to zero,

$$\frac{\partial S}{\partial \hat{A}} = 0 \qquad ,j=1,2,\ldots,M \qquad \ldots(4.1.3)$$

The resulting normal equation will be of the form

$$(\underline{A}^t A)\,\Delta\hat{A} = \underline{A}^t\,(y-\hat{y}^*) \qquad .....(4.1.4)$$

$$\underline{A} = \begin{bmatrix} \frac{\partial \hat{y}_1}{\partial \hat{A}_1} & \frac{\partial \hat{y}_1}{\partial \hat{A}_2} & \cdots\cdots\cdots\cdots & \frac{\partial \hat{y}_1}{\partial \hat{A}_M} \\ \frac{\partial \hat{y}_2}{\partial \hat{A}_1} & \frac{\partial \hat{y}_2}{\partial \hat{A}_2} & \cdots\cdots\cdots\cdots & \frac{\partial \hat{y}_2}{\partial \hat{A}_M} \\ \cdot & & & \\ \cdot & & & \\ \frac{\partial \hat{y}_M}{\partial \hat{A}_1} & \frac{\partial \hat{y}_M}{\partial \hat{A}_2} & \cdots\cdots\cdots\cdots & \frac{\partial \hat{y}_M}{\partial \hat{A}_M} \end{bmatrix}^*$$

$$\Delta\hat{\underline{A}} = \begin{bmatrix} (\hat{A}_1 - \hat{A}_1^*) \\ (\hat{A}_2 - \hat{A}_2^*) \\ \cdot \\ \cdot \\ (\hat{A}_M - \hat{A}_M^*) \end{bmatrix} \qquad (y - \hat{y}^*) = \begin{bmatrix} (y_1 - \hat{y}_1^*) \\ (y_2 - \hat{y}_2^*) \\ \cdot \\ \cdot \\ (y_N - \hat{y}_N^*) \end{bmatrix}$$

$\underline{A}^t$ is the transpose of the $\underline{A}$ matrix. The derivative in the $\underline{A}$ matrix may be evaluated analytically or numerically.

4.1.4 The normal equations are a system of linear algebraic equations and are solved by a appropriate technique for $\Delta\hat{\underline{A}}$. The $\Delta\hat{\underline{A}}$ vector and S will approach zero as convergence is achieved. If convergence is achieved, the final coefficients are calculated from

$$\hat{A}_j = \hat{A}_j^* + \Delta\hat{A}_j \qquad ,j=1,2,....,M \qquad ...(4.1.5)$$

If convergence is not achieved $\hat{\underline{A}}^*$ is updated by replacing the old values by the new values and the process is repeated.

A flow sheet illustrating the above procedure is given as

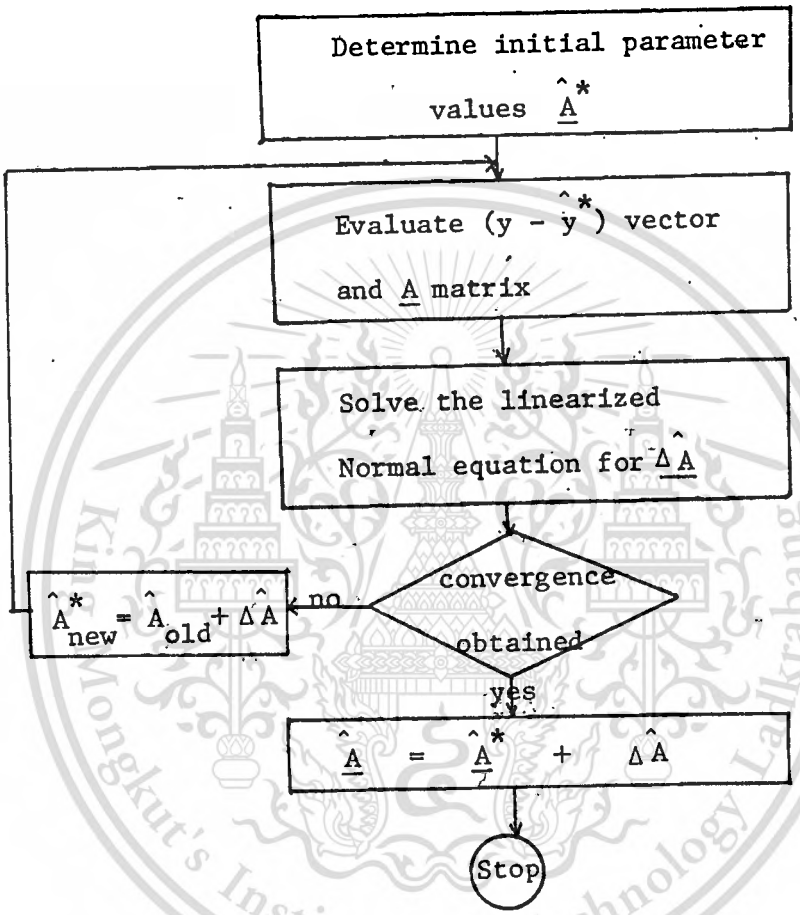

Fig 4.1 Flow chart of Gauss-Newton Algorithm.

For this problem, the objective function is a least-square form.

$$S = \sum^{k} (y_k - \hat{y}_k)^2 \qquad .....(4.1.6)$$

where k = number of data points

y_k = discrete data points

$\hat{y}_k$ = value of the function to be minimized, in this case is the sum of four lorentzian functions.

$$\hat{y}_k = \sum_{i=1}^{4} \frac{A_i a_i (H - H_{0i})}{(a_i^2 + (H-H_{0i})^2)^2} \qquad .....(4.1.7)$$

The physical problem being studied has the following conditions. Each lorentzian function has three variables, so there are a total of 12 variables. Let

$a_i = A_i$; i=1,2,3,4 Amplitude of individual lines.

$a_j = A_j$; j=5,6,7,8 Width of individual lines.

$a_k = A_k$; k=9,10,11,12 Positive(in step) of centre of the individual.

We do this problem following the 4 processes outlined in section 4.1.1, 4.1.2, 4.1.3, 4.1.4 and

$$A = \begin{bmatrix} \frac{\partial \hat{y}_1}{\partial a_1} & \frac{\partial \hat{y}_1}{\partial a_2} & \cdots\cdots\cdots\cdots\cdots & \frac{\partial \hat{y}_1}{\partial a_{12}} \\ \cdot & & & \\ \cdot & & & \\ \cdot & & & \\ \frac{\partial \hat{y}_{12}}{\partial a_1} & \frac{\partial \hat{y}_{12}}{\partial a_2} & & \frac{\partial \hat{y}_{12}}{\partial a_{12}} \end{bmatrix} \qquad ....(4.1.8)$$

$$(y - \hat{y}^*) = \begin{bmatrix} (y_1 - \hat{y}_1^*) \\ \\ \\ (y_{12} - \hat{y}_{12}^*) \end{bmatrix} \qquad .....(4.1.9)$$

$$\underline{\Delta\hat{A}} = \begin{bmatrix} (a_1 - \hat{a}_1^*) \\ \\ \\ (a_{12} - \hat{a}_{12}^*) \end{bmatrix} \qquad \ldots\ldots(4.1.10)$$

$$\hat{y}_i = \hat{y}_i^* + \left[\frac{\partial \hat{y}_i}{\partial a_1}\right]^* \Delta a_1 + \left[\frac{\partial \hat{y}_i}{\partial a_2}\right]^* \Delta a_2 + \ldots\ldots + \left[\frac{\partial \hat{y}_i}{\partial a_{12}}\right]^* \Delta a_{12} \quad \ldots(4.1.1$$

$$\Delta a_j = (a_j - a_j^*) \qquad j=1,2,\ldots\ldots\ldots,12 \qquad (4.1.1$$

The final result is $a_1, a_2, \ldots\ldots, a_{12}$; the values of the variables giving a minimum value of the function.

4.2. Gradient Projection Algorithm

The objective function is denoted by $f(\hat{y})$ (in our case the sum of four lorentzian functions, each function has three variables A, a, H_0) where y is a 12-dimensional variables;

$y_i = A_i$; i=1,2,3,4 Amplitude of line shape.

$y_j = A_j$; j=5,6,7,8 Width of individual line.

$y_k = A_k$; k=9,10,11,12 Position(in step) of centre of the individual line.

The 12-variables $(A_i, a_i, H_{0i}$; i=1,2,.....,12) are contrained by 24 linear inequalities of the form

$$b_i \leqslant y_i \leqslant c_i \qquad \ldots(4.2.1)$$

so that

$$y_i - b_i \geqslant 0 \qquad i=1,2,\ldots\ldots\ldots,12 \qquad \ldots(4.2.2)$$

$$-y_i + c_i \geqslant 0 \qquad i=1,2,\ldots\ldots\ldots,12 \qquad \ldots(4.2.3)$$

b_i is the lower bound on y_i

c_i is the upper bound on y_i

One can see that a feasible region is bounded by 24 hyperplanes.

Suppose that $\hat{y}$ is a point that lies in the intersection of q

These hyperplanes, which for convenience we shall assume are $H_1, H_2, \ldots\ldots, H_q$ are defined by q linearly independent unit normals $\hat{n}_1, \hat{n}_2, \ldots\ldots\ldots, \hat{n}_q$ ($\hat{n}_i$ is a 12-dimension vector ; all elements are zero expept one is 1 or -1 for example $\hat{n}_1 = [1,0,0,..,0]^T$) and the components $V_1, V_2, \ldots\ldots, V_q$ of vector V (v_i is b or c)

$$\begin{bmatrix} 1 & 0 & 0 & 0 & \ldots\ldots & -1 & 0 & 0 & 0 & \ldots\ldots \\ 0 & 1 & 0 & 0 & \ldots\ldots & 0 & -1 & 0 & 0 & \ldots\ldots \\ 0 & 0 & 1 & 0 & \ldots\ldots & 0 & 0 & -1 & 0 & \ldots\ldots \\ \ldots\ldots & & & & & & & & & \ldots\ldots \\ & & & 1 & & & & -1 & & \end{bmatrix}^T \begin{bmatrix} y_1 \\ y_2 \\ y_3 \\ \vdots \\ y_{12} \end{bmatrix} - \begin{bmatrix} b_1 \ldots b_{12} c_1 \ldots c_{12} \end{bmatrix}^T = 0 \qquad \ldots(4.2.5)$$

or representation in this form

$$\begin{bmatrix} n_1, n_2, \ldots\ldots, n_q \end{bmatrix}^T Y - \begin{bmatrix} v_1, v_2, \ldots\ldots, v_q \end{bmatrix}^T \triangleq N_q^T Y - V_q = 0 \qquad \ldots(4.2.6)$$

It is assumed that the partial derivatives of the objective function are known

if $\frac{\partial f^{(i)}}{\partial y}$ is the gradient at the point $\hat{Y}^{(i)}$ ($\hat{Y}^{(i)} = [\hat{y}_1^i, \hat{y}_2^i \ldots \hat{y}_{12}^i]^T$)

$-\frac{\partial f^{(i)}}{\partial y}$ is obtained by changing the sign of each component of $\frac{\partial f^{(i)}}{\partial y}$

step 1 The projection matrix (12×12 symmetric matrix) is formed by

$$P_q = I - N_q \left[N_q^T N_q\right]^{-1} N_q^T \qquad \ldots(4.2.7)$$

(projection matrix is a matrix of a projection of $\frac{\partial f^{(i)}}{\partial y}$)

if y lies in the interior of the admissible region, the projection matrix at $\hat{y}^{(i)}$ is the identity matrix. If $\| P_q (-\frac{\partial f^{(i)}}{\partial y}) \| < \varepsilon$

and $r \leq 0$ ($r = \left[N_q^T N_q\right]^{-1} N_q \left(-\left[\frac{\partial f^{(i)}}{\partial y}(y)\right]\right)$), then $\hat{y}^{(i)}$ is the global minimum and the proceduce is terminated; otherwise go to step 2

step 2 Determine whether or not a hyperplane should be dropped from Q

If $\left|\left| P_q \left(-\left[\frac{\partial f^{(i)}}{\partial y}\right]\right)\right|\right| < \varepsilon_1$,drop the hyperplane H_q ,which corresponds to $r_q > 0$, form the projection matrix P_{q-1} and go to step 3. The other alternative is that the norm of the gradient projection is greater than ε . In this case,calculate β (let $\alpha_i \triangleq$ the sum of the absolute values of the elements of the i^{th} row of the matrix $\left[N_q^T N_q\right]^{-1}$,calculate α_i ,i=1,2,....,q an determine $\beta = \max(\alpha_i)$. If $r_q > \beta$, drop the hyperplane H_q from Q ; if $r_q < \beta$,Q remains unchanged.

step 3 The maximum allowable step size

In changing $\vec{y}^{(i)}$ in the direction of projected gradient,it is necessary to know the maximum stepsize that can be used without causing any of the constraints to be violated.

$$\text{Let } Z^{(i)} = P_q \left(-\left[\frac{\partial f^{(i)}}{\partial y}\right]\right) \Big/ \left|\left| P_q \left(-\left[\frac{\partial f^{(i)}}{\partial y}\right]\right)\right|\right| \quad ...(4.2.8)$$

and define

$$\vec{y}'^{(i+1)} \triangleq \vec{y}^{(i)} + \tau \vec{Z}^{(i)} \quad ...(4.2.9)$$

where τ is a scalar that represents the step size.

Let

$$\vec{y}_j'^{(i+1)} = \vec{y}^{(i)} + \tau_j \vec{Z}^{(i)} \quad ...(4.2.10)$$

be the point where this line intersects the hyperplane H_j (H_j not in Q subspace) ; then

$$n_j^T \vec{y}_j'^{(i+1)} - V_j = 0 \quad ...(4.2.11)$$

Substituting $y_j'^{(i+1)}$ from equation(4.2.11) which when solved for τ_j yields.

$$\tau_j = \frac{V_j - n_j^T \vec{y}^{(i)}}{n_j^T \vec{Z}^{(i)}} \quad ...(4.2.12)$$

The minimum position value of these τ_j s , denoted by τ_m determines the maximum step that can be taken along the line from equation (4.2.8) without violating any constraints.

$$\vec{y}'^{(i+1)} = \vec{y}^{(i)} + \tau_m \vec{Z}^{(i)} \quad ...(4.2.1.)$$

4.2.1. Interpolation

To determine whether or not the maximum step size should be used, we form the inner product.

$$\vec{Z}^{(i)T} \left(- \frac{\partial f(\vec{y}^{(i+1)})}{\partial y} \right) \quad \ldots(4.2.14)$$

If this inner product is greater than or equal to zero, H_m is added, and the new.

Projection matrix P_{q+1} is calculated. On the other hand, if the inner product is negative, the maximum step is not taken. Instead, interpolation is used to find the point.

$$\vec{y}^{(i+1)} = \vec{y}^{(i)} + \theta T_m \vec{Z}^{(i)} \quad \ldots(4.2.15)$$

$$(\quad 0 < \theta < 1)$$

where

$$\vec{Z}^{(i)T} \left(- \left[\frac{\partial f(\vec{y}^{(i+1)})}{\partial y} \right] \right) = 0 \quad \ldots(4.2.16)$$

or for practical purposes

$$\left| Z^{(i)T} \left(- \left[\frac{\partial f^{(i+1)}}{\partial y} \right] \right) \right| = \varepsilon_2 \quad \ldots(4.2.17)$$

ε_2 is a preassigned small positive number. After getting $y^{(i+1)}$ returning to step 1

The objective matrix in this case is = S

$$S = \sum^{K} (y_k - \hat{y}_k) \quad \ldots(4.2.18)$$

K = number of data points.

y_k = a discrete data points.

y_k = the sum of four lorentzians.

$$= \sum_{i=1}^{4} \frac{A_i a_i (H - H_{0i})}{(a_i^2 + (H - H_{0i})^2)^2} \quad \ldots(4.2.19)$$

So there are twelve variables (A_i , a_i , H_{0i} ; i=1,2,3,4) which have constraints.

$$b_0 \leq A_i \leq b_1$$

$$c_0 \leq a_i \leq c_1$$

$$d_0 \leq H_{0i} \leq d_1 \quad \ldots(4.2.20)$$

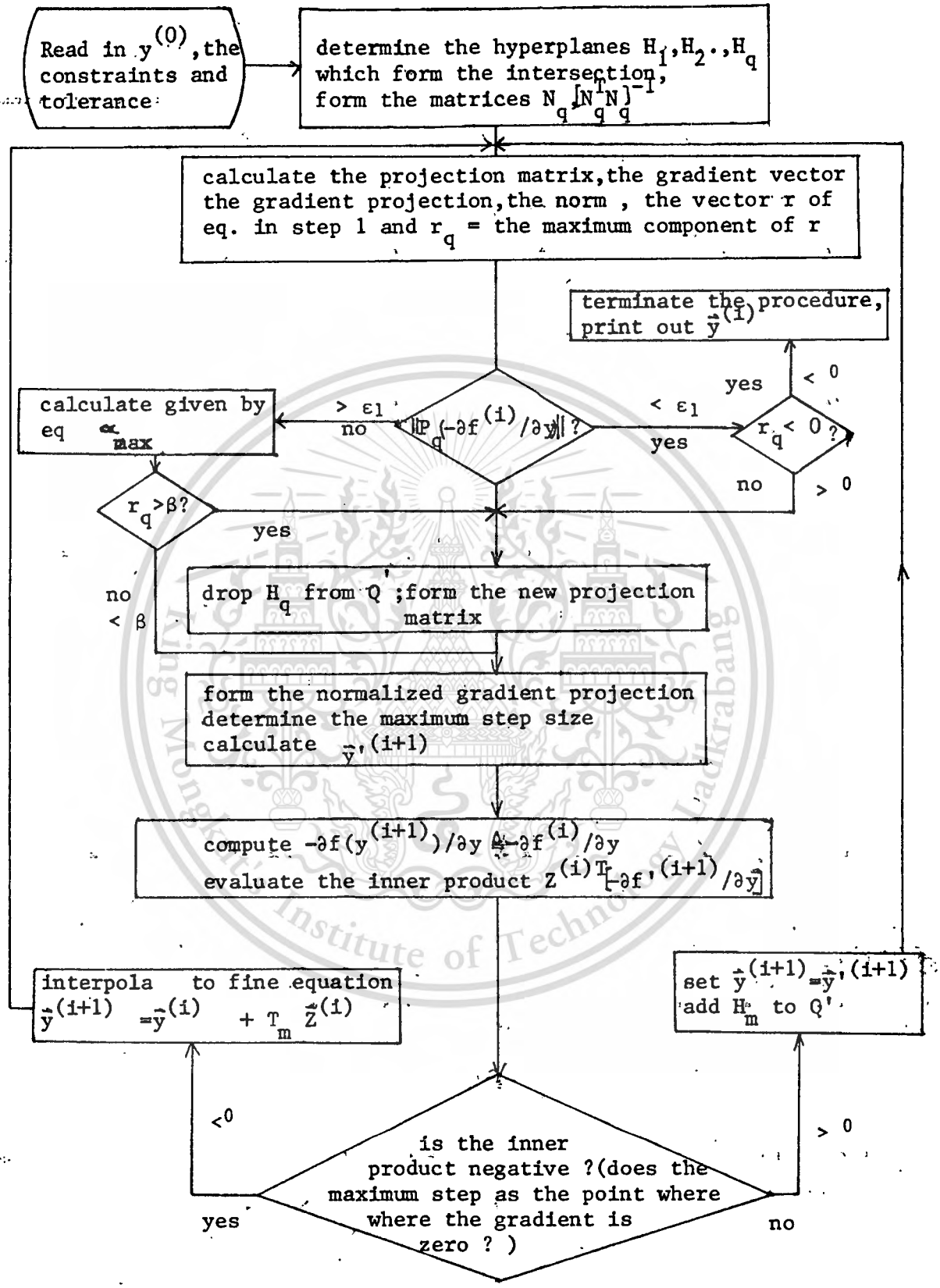

Fig 4.2 Flow chart of Gradient Projection Algorithm.

We have 24 constraint relations:

$$A_1 = b_0 \;,\; a_1 = c_0 \;,\; H_{01} = d_0$$
$$A_1 = b_1 \;,\; a_1 = c_1 \;,\; H_{01} = d_1$$
$$A_2 = b_0 \;,\; a_2 = c_0 \;,\; H_{02} = d_0$$
$$A_2 = b_1 \;,\; a_2 = c_1 \;,\; H_{02} = d_1$$
$$A_3 = b_0 \;,\; a_3 = c_0 \;,\; H_{03} = d_0$$
$$A_3 = b_1 \;,\; a_3 = c_1 \;,\; H_{03} = d_1$$
$$A_4 = b_0 \;,\; a_4 = c_0 \;,\; H_{04} = d_0$$
$$A_4 = b_1 \;,\; a_4 = c_1 \;,\; H_{04} = d_1 \qquad \ldots.(4.2.20)$$

The adventage of the gradient projection method over the gauss-newton method is its flexibility of initial conditions in the admissible region. So the starting point in iteration could be chosen arbitraly (as long as it occurs in the feasible region) , because this algorithm will always converge to local minimum points.

4.3 Results.

The resuts of the calculation with 6 variables are showned in Fig 4.1.1-4.1.8. The values ofvvariables are showned in table 4.1.1.

The results of the calculation with 12 variables are showned in Fig 4.2.1-4.2.8 . The values of variables are showned in table 4.2.1

The results of the calculation wi h 3 variables are showned in Fig 4.3.1-4.3.8. The values of variables are showned in table 4.3.1.

Fig 4.4.1 is the plotting of 1/T againt T.

Table 4.1.1 Calculation with 6 variables.

	1 76.4	2 77.0	3 80.2	4 84.0	5 92.2	6 102.8	7 110.4	8 77.0
A	5690.40	821.99	3499.00	3705.48	3633.42	2852.26	2940.68	6367.30
a_1	11.658	4.145	14.720	9.522	9.220	8.850	8.787	10.254
a_2	9.679	5.506	16.760	15.469	19.230	16.378	15.669	13.130
a_3	18.607	7.660	27.670	21.710	17.850	14.574	16.729	15.690
a_4	14.819	10.220	28.510	16.930	17.350	16.756	13.167	18.040
ΔH	8.330	9.090	6.900	7.010	6.550	7.174	5.810	23.937

Table 4.3.1 Calculation with 3 variables.

	1 76.4	2 77.0	3 80.2	4 84.0	5 92.2	6 102.8	7 110.4	8 77.0
A	7606.15	788.817	3499.00	4387.11	4140.87	3258.44	3682.99	5391.58
a_1	11.670	3.986	13.183	10.181	9.455	8.874	9.772	8.994
a_2	$1.59a_1$	$1.59a_1$	$1.59a_1$	$1.59a_1$	$1.59a_1$	$1.59a_1$	$1.59a_1$	$1.37a_1$
a_3	$2.33a_1$	$2.33a_1$	$2.33a_1$	$2.33a_1$	$2,33a_1$	$2.33a_1$	$2.33a_1$	$1.79a_1$
a_4	$3.16a_1$	$3.16a_1$	$3.16a_1$	$3.16a_1$	$3.16a_1$	$3.16a_1$	$3.16a_1$	$3.16a_1$
ΔH	8.170	9.125	7.896	9.050	9.732	9.965	7.896	23.647

Table 4.2.1 Calculation with 12 variables.

.	1	2	3	4	5	6	7	8
K	76.4	77.0	80.2	84.0	92.2	102.8	110.4	77.0
A_1	5690.00	885.12	3499.9	3705.48	3633.00	5205.00	2940.00	5835.00
A_2	5690.00	693.39	3499.68	3705.48	3633.00	3258.00	2940.00	6752.59
A_3	5690.00	935.70	3499.41	3705.48	3633.00	3260.00	2940.00	7088.89
A_4	5690.00	856.02	3499.27	3705.48	3633.00	3251.00	2940.00	6039.18
a_1	12.225	4.099	19.681	9.387	9.151	13.723	8.630	9.782
a_2	9.913	5.205	12.306	15.207	18.404	10.000	14.770	13.689
a_3	17.143	8.608	24.129	21.719	17.073	14.192	16.620	16.576
a_4	15.678	11.159	27.044	17.198	17.227	25.059	14.170	17.538
H_{01}	60.535	18.173	42.185	48.926	41.236	45.037	38.451	43.942
H_{02}	67.784	27.622	49.895	56.545	48.402	36.870	45.234	67.971
H_{03}	78.037	36.665	52.486	63.718	54.777	55.761	50.746	92.219
H_{04}	86.158	46.046	62.885	70.742	61.950	61.454	57.438	116.045

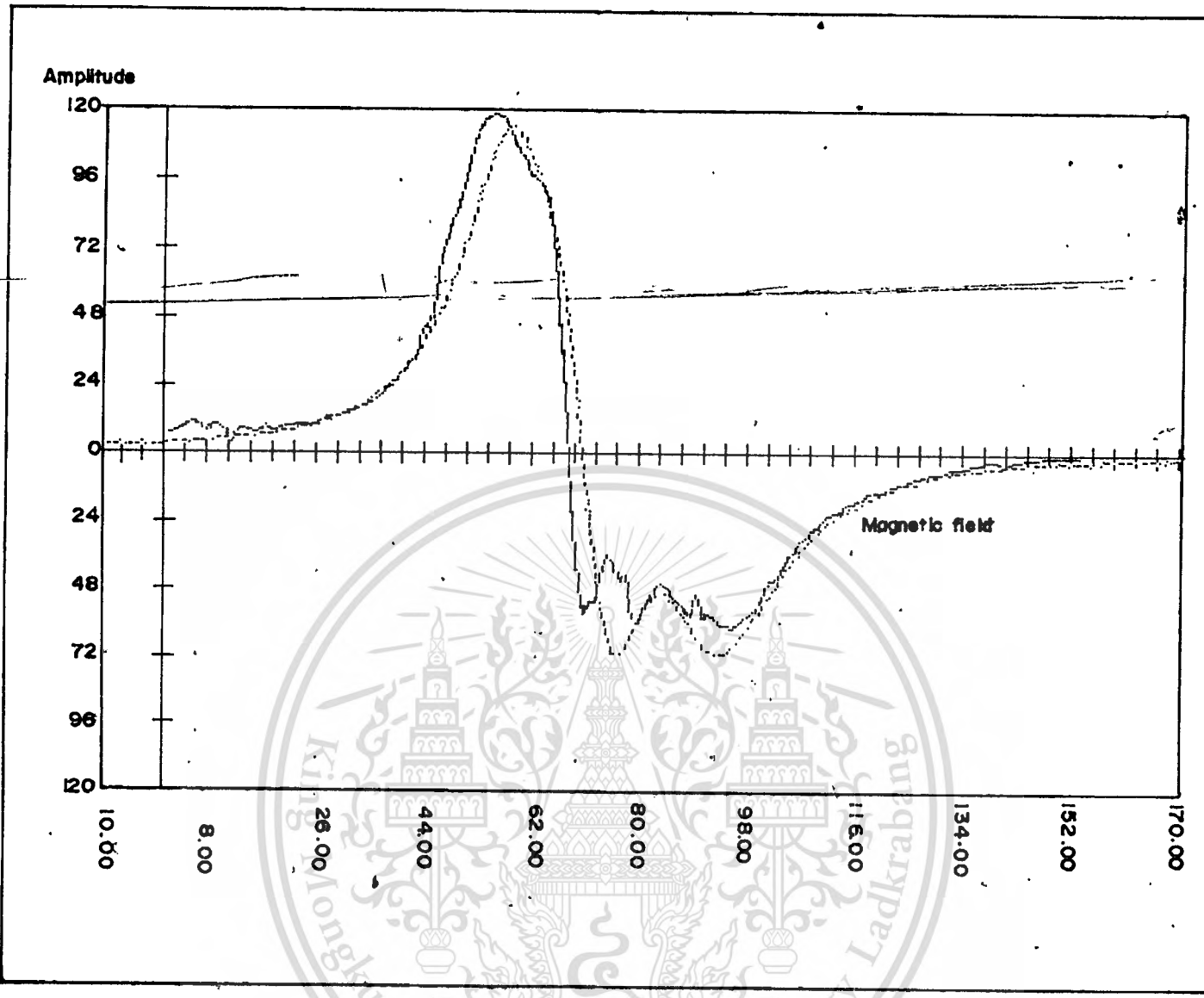

Figure 4.1.1. EXPERIMENTAL AND COMPUTED CURVES USING GAUSS NEWTON WITH 6 VARIABLES (ARBITRARY SCALE UNITS) ; —— EXPERIMENTAL CURVE, ...COMPUTED CURVE AT TEMPERATVRE 76.4 K

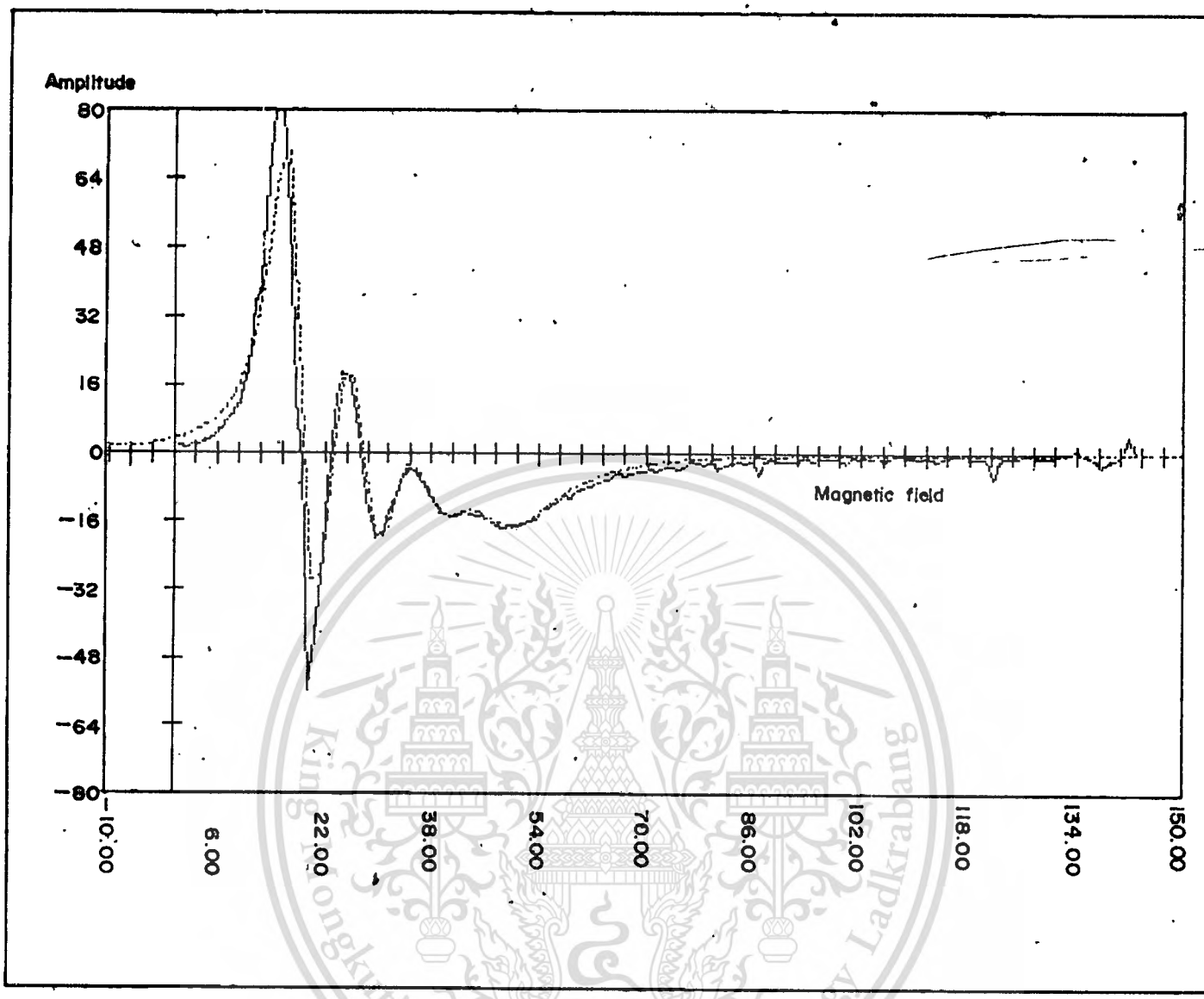

Figure 4·1·2. EXPERIMENTAL AND COMPUTED CURVES USING GAUSS-NEWTON WITH 6 VARIABLES (ARBITRARY SCALE UNITS); —— EXPERIMENTAL CURVE, ····· COMPUTED CURVE AT TEMPERATURE 77°K

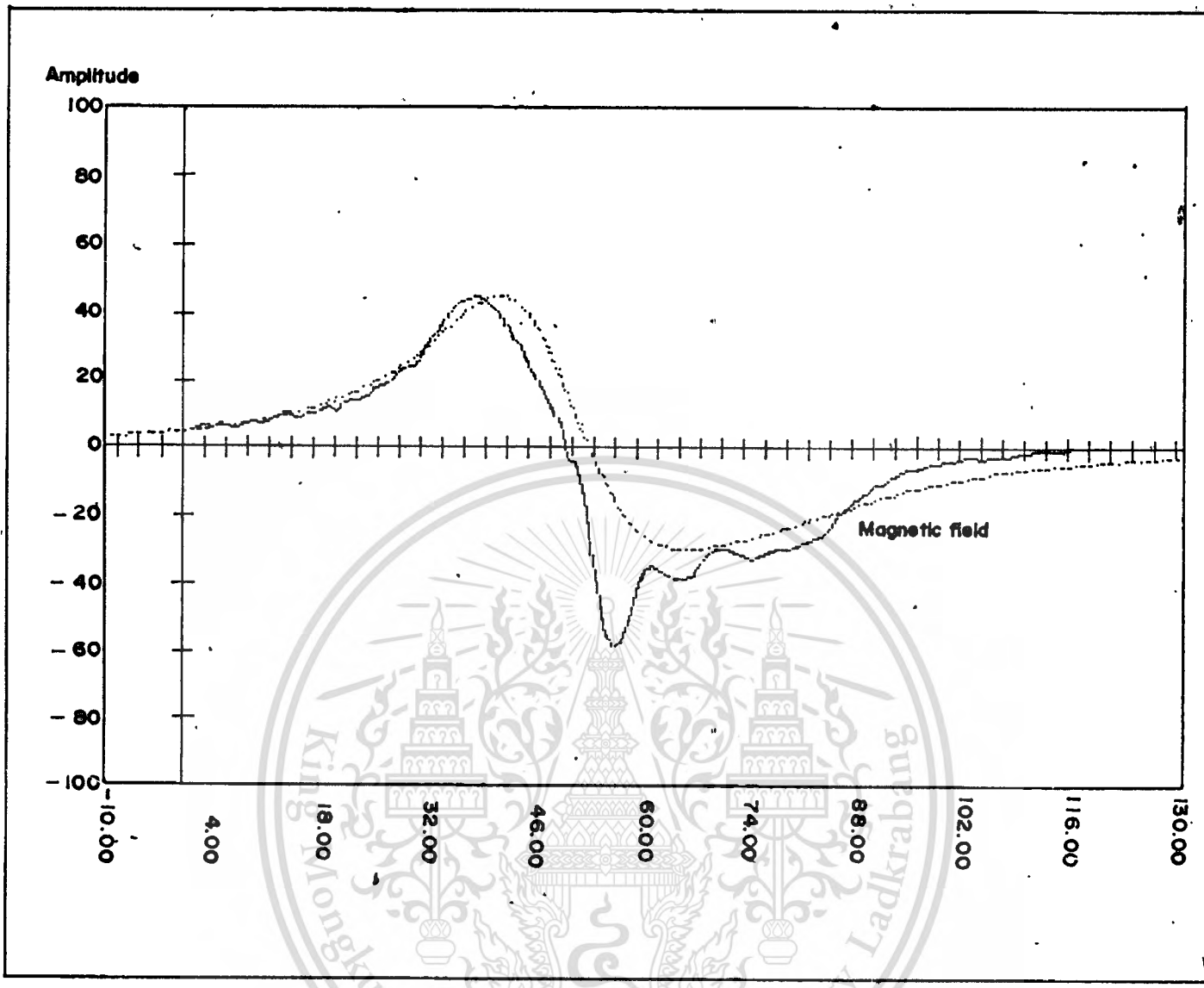

Figure 4.1.3. EXPERIMENTAL AND COMPUTED CURVES USING GAUSS NEWTON WITH 6 VARIABLES (ARBITRARY SCALE UNITS) ; —— EXPERIMENTAL CURVE, ... COMPUTED CURVE AT TEMPERATURE 80.2 K

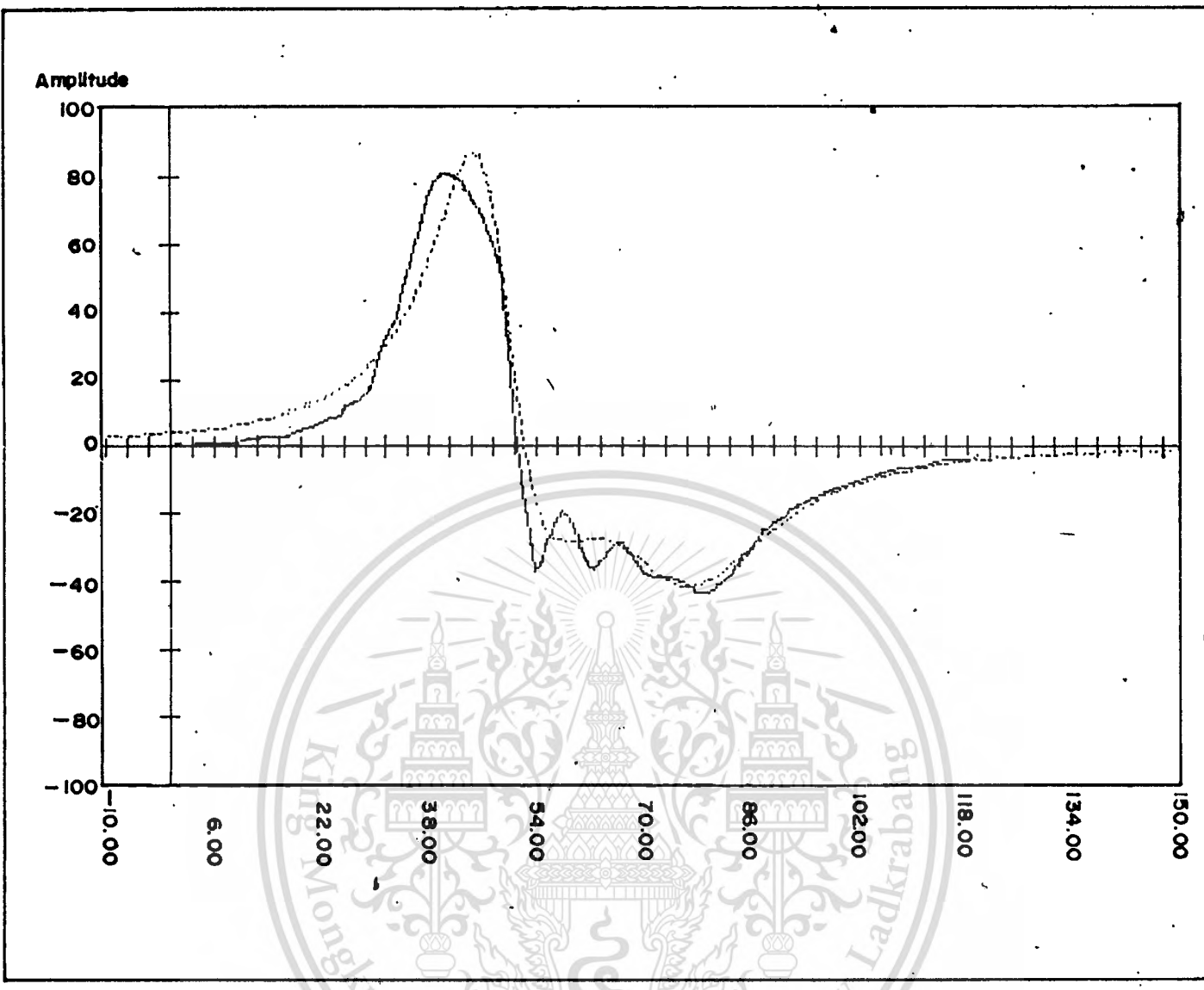

Figure 4.1.4. EXPERIMENTAL AND COMPUTED CURVES USING GAUSS NEWTON WITH 6 VARIABLES (ARBITRARY SCALE UNITS) ; —— EXPERIMENTAL CURVE, ... COMPUTED CURVE AT TEMPERATURE 84° K

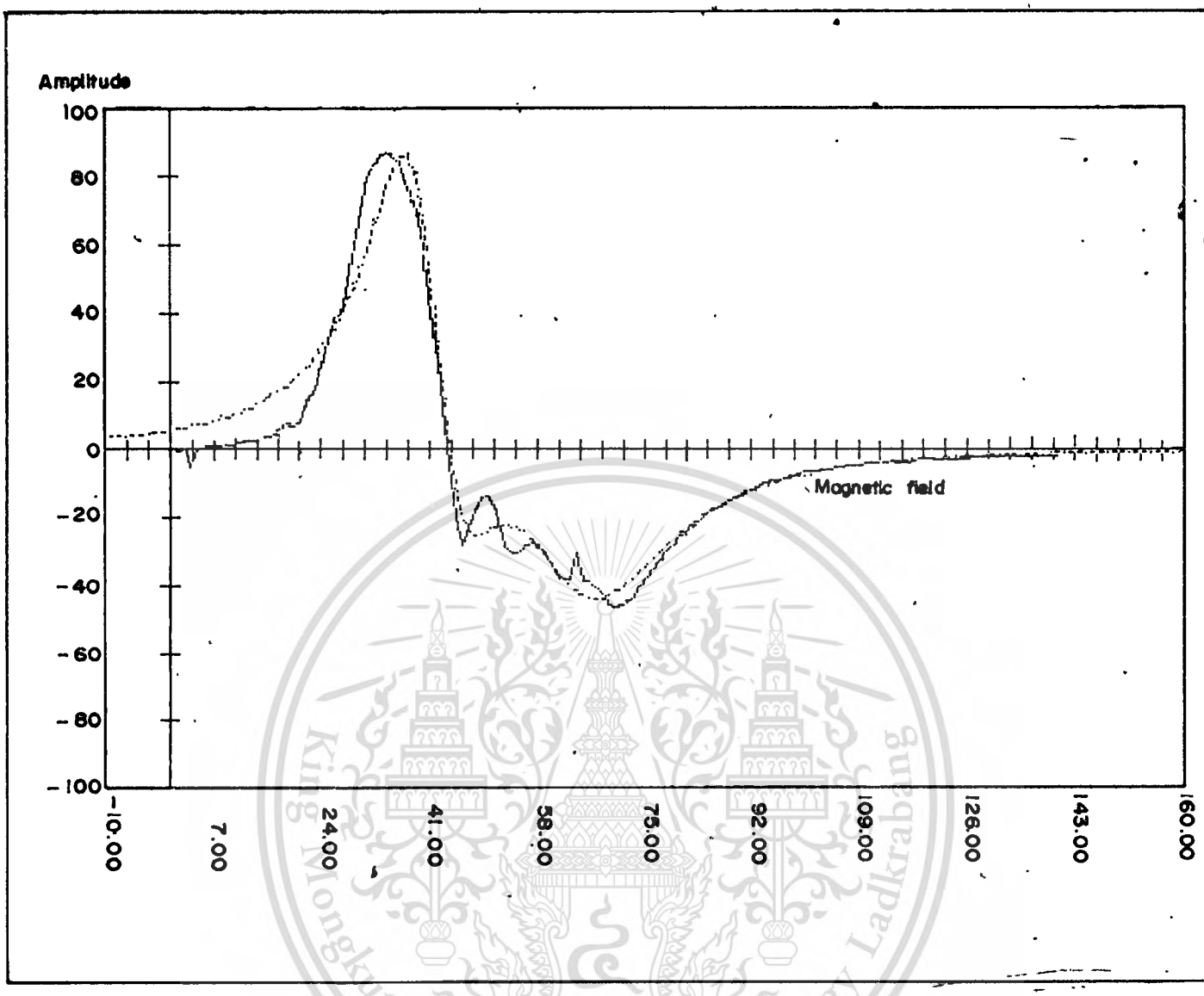

Figure 4.1.5 EXPERIMENTAL AND COMPUTED CURVES USING GAUSS NEWTON WITH 6 VARIABLES (ARBITRARY SCALE UNITS) ; —— EXPERIMENTAL CURVE, ------ COMPUTED CURVE AT TEMPERATVRE 92.2° K

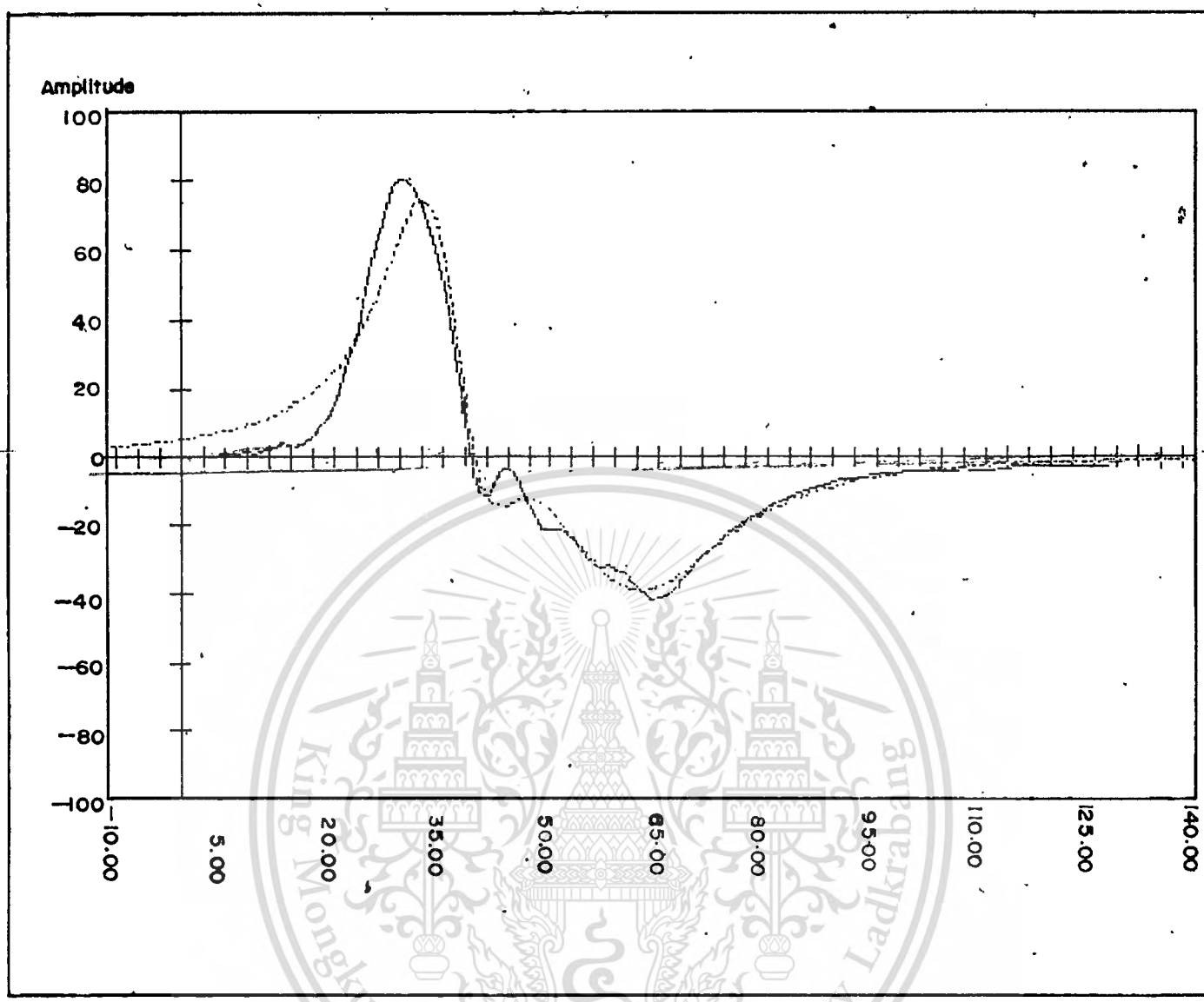

Figure 4.1.6. EXPERIMENTAL AND COMPUTED CURVES USING GAUSS NEWTON WITH 6 VARIABLES. (ARBITRARY SCALE UNITS); —— EXPERIMENTAL CURVE, ... COMPUTED CURVE AT TEMPERATURE 102.8 °K

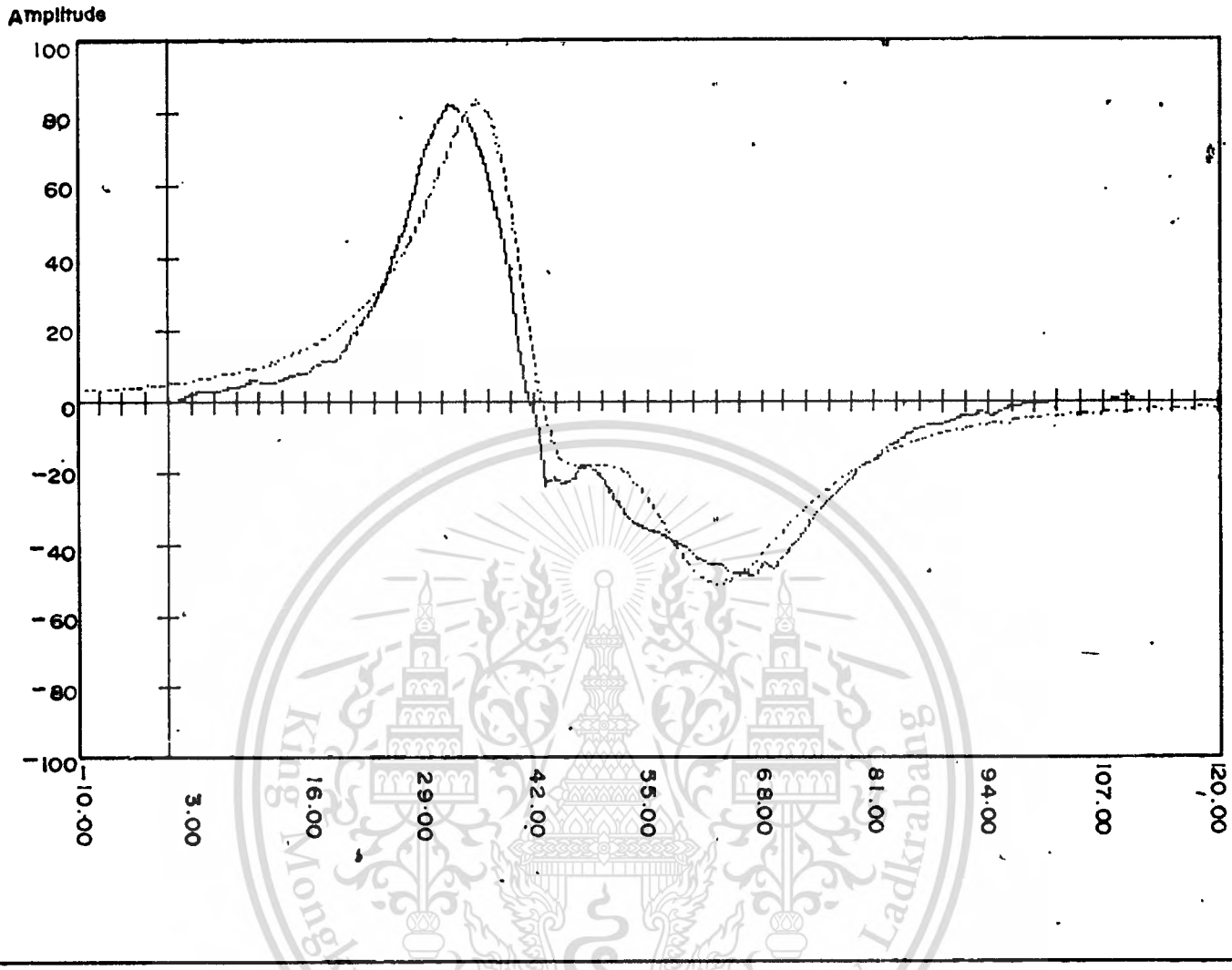

Figure 4.1.7. EXPERIMENTAL AND COMPUTED CURVES USING GAUSS NEWTON WITH 6 VARIABLES (ARBITRARY SCALE UNITS); EXPERIMENTAL CURVE, ... COMPUTED CURVE AT TEMPERATURE 110.4°K

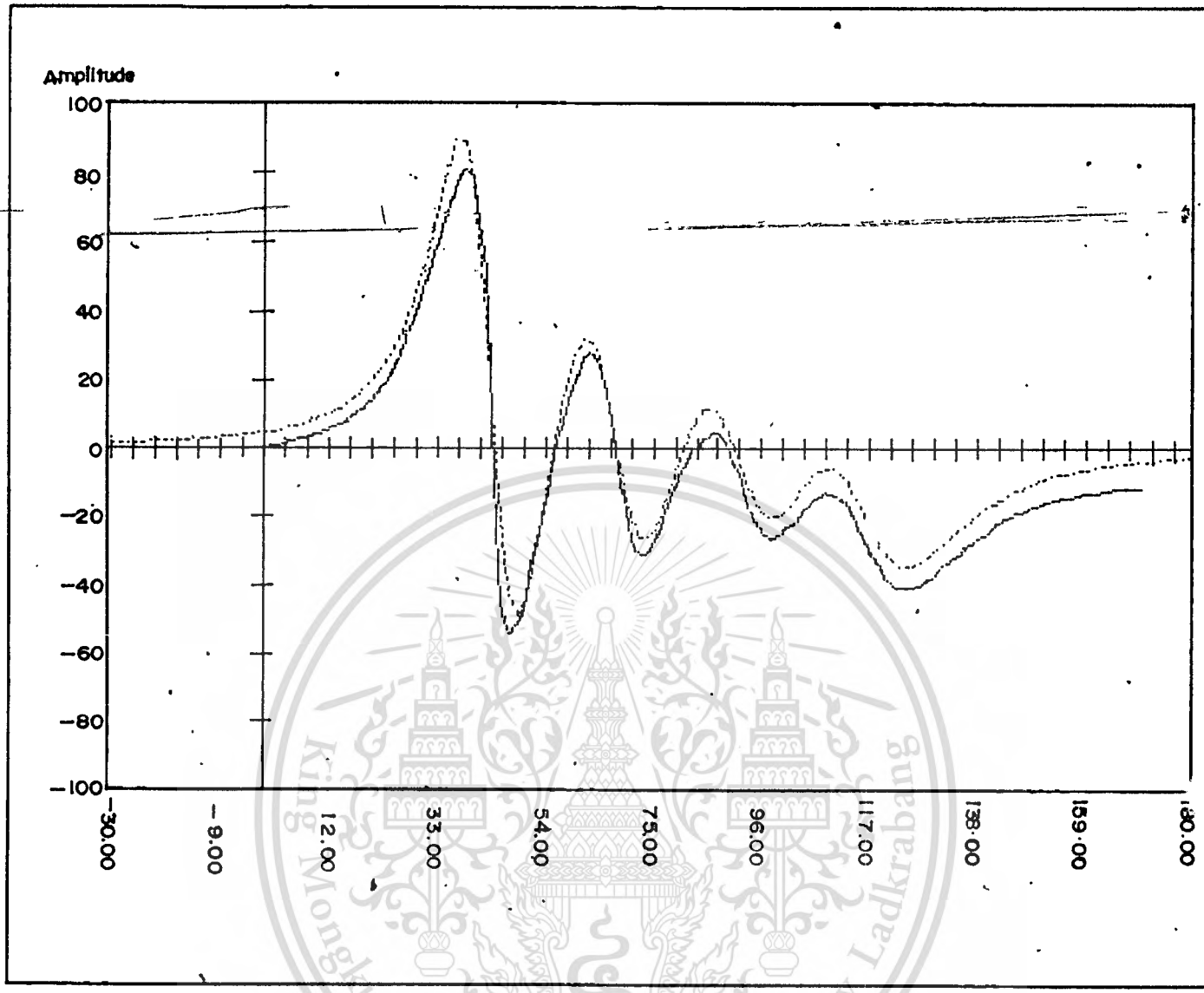

Figure 4.1.8. EXPERIMENTAL AND COMPUTED CURVES USING GAUSS NEWTON WITH 6 VARIABLES (ARBITRARY SCALE UNITS) ; —— EXPERIMENTAL CURVE, ... COMPUTED CURVE AT TEMPERATURE 77°K

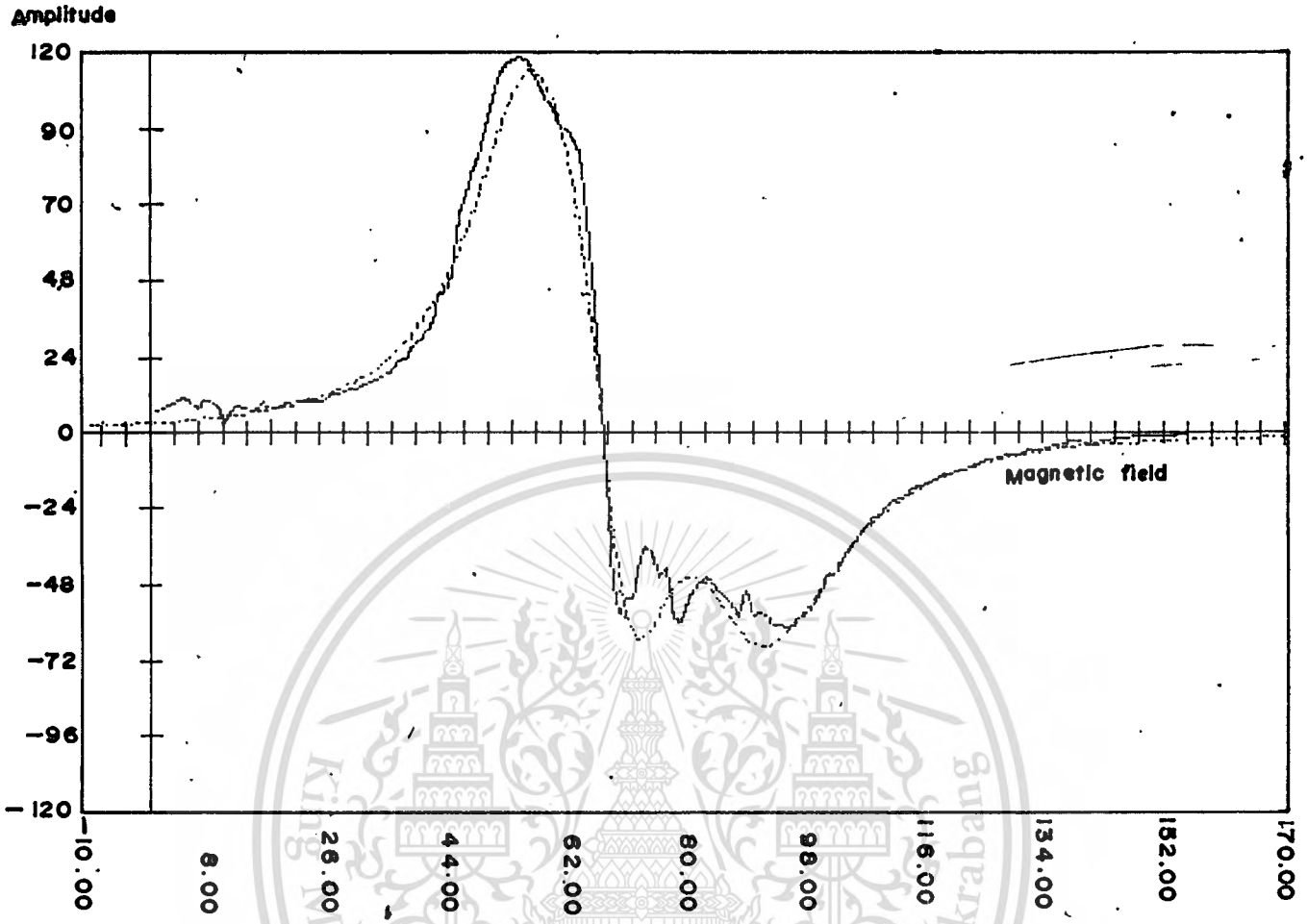

Figure 4.2.3. EXPERIMENTAL AND COMPUTED CURVES USING GRADIENT PROJECTION WITH 12 VARIABLES (ARBITRARY SCALE UNITS) ; —— EXPERIMENTAL CURVE, ····· COMPUTED CURVE AT TEMPERATURE 76.4 °K

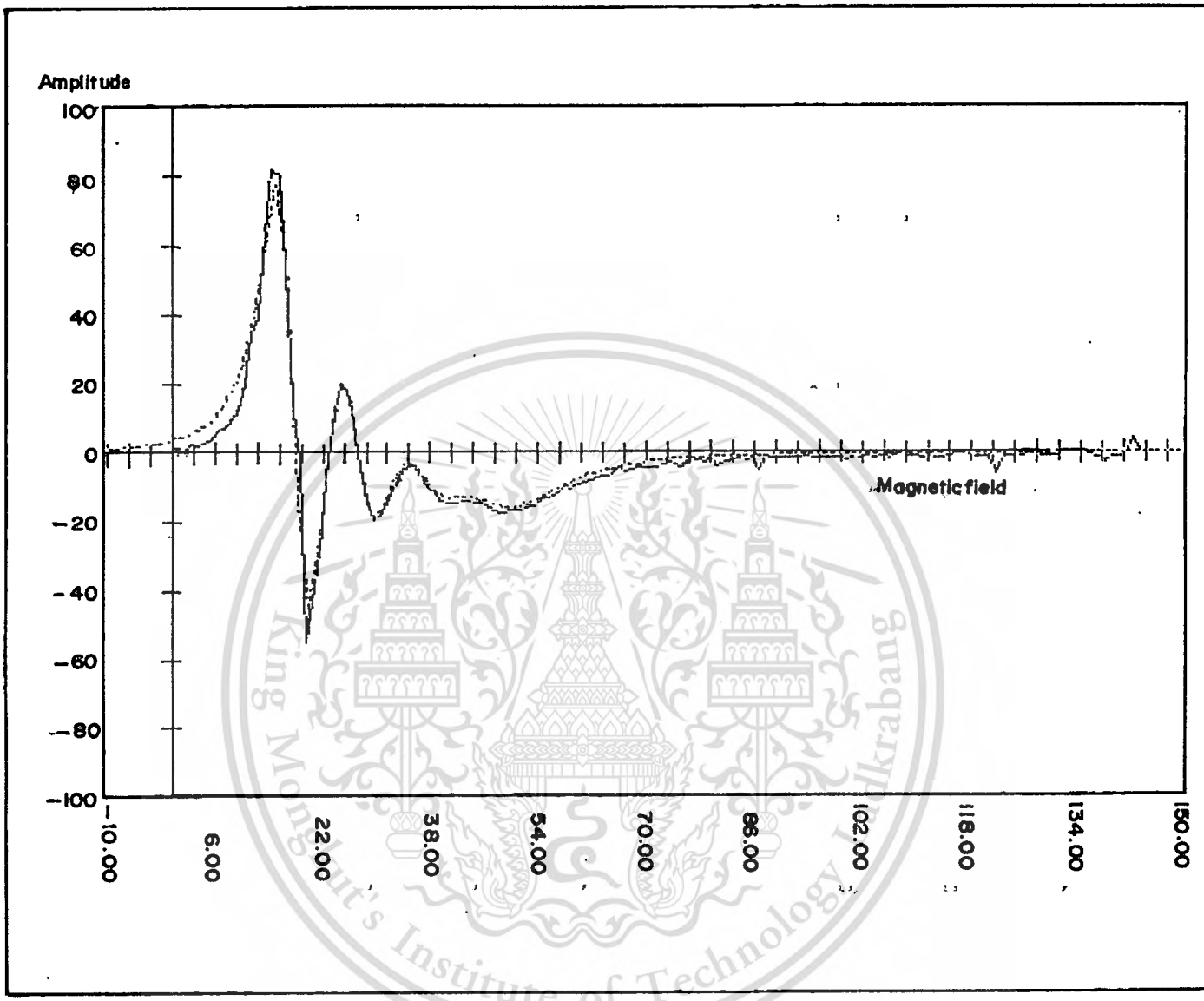

Figure 4.2.2 EXPERIMENTAL AND COMPUTED CURVES USING GRADIENT PROJECTION WITH 12 VARIABLES (ARBITRARY SCALE UNITS) ; —— EXPERIMENTAL CURVE , ... COMPUTED CURVE AT TEMPERATURE 77°K

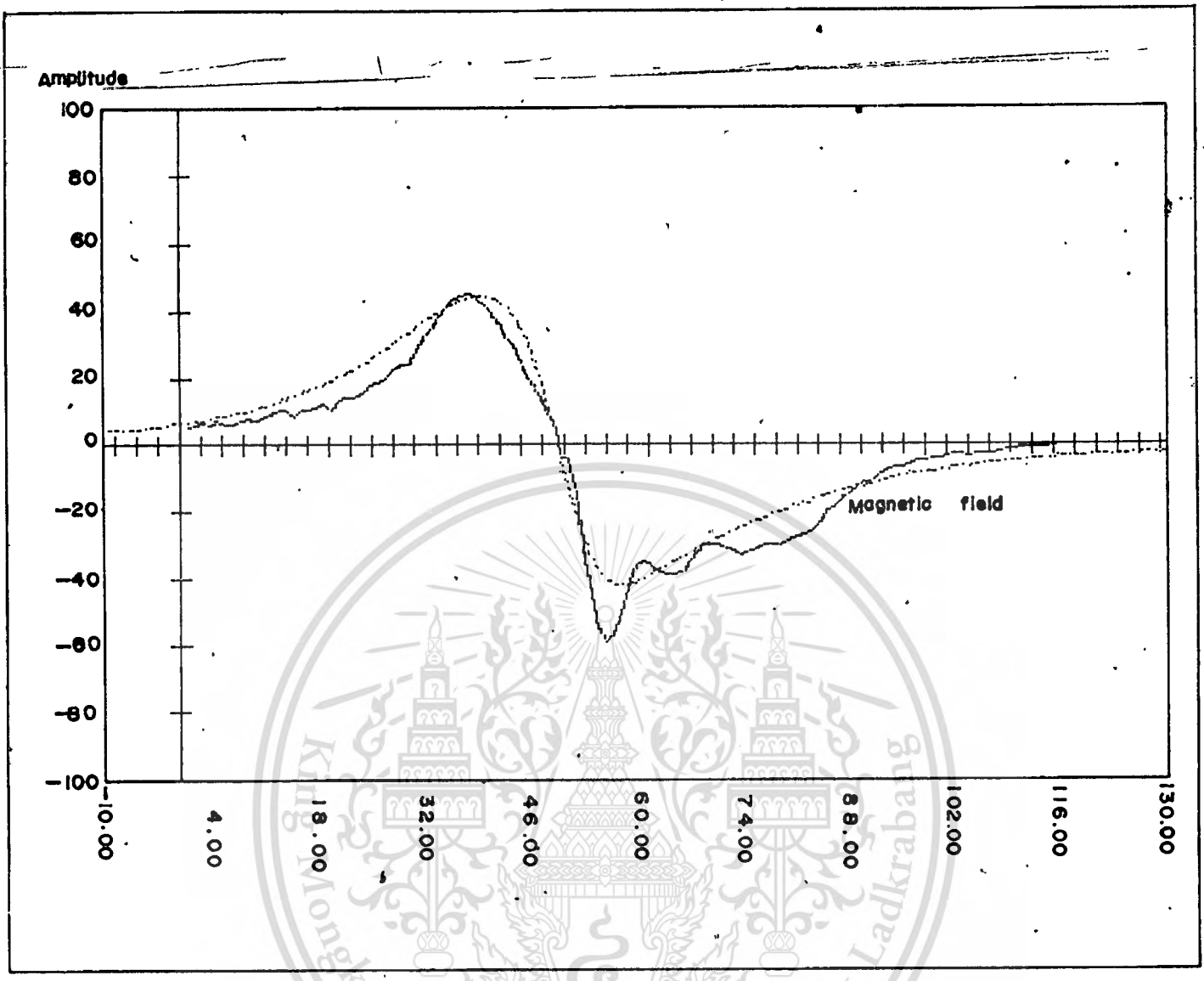

Figure 4.2.3. EXPERIMENTAL AND COMPUTED CURVES USING GRADIENT PROJECTION WITH 12 VARIABLES (ARBITRARY SCALE UNITS); —— EXPERIMENTAL CURVE, ------ COMPUTED CURVE AT TEMPERATURE 80.2° K

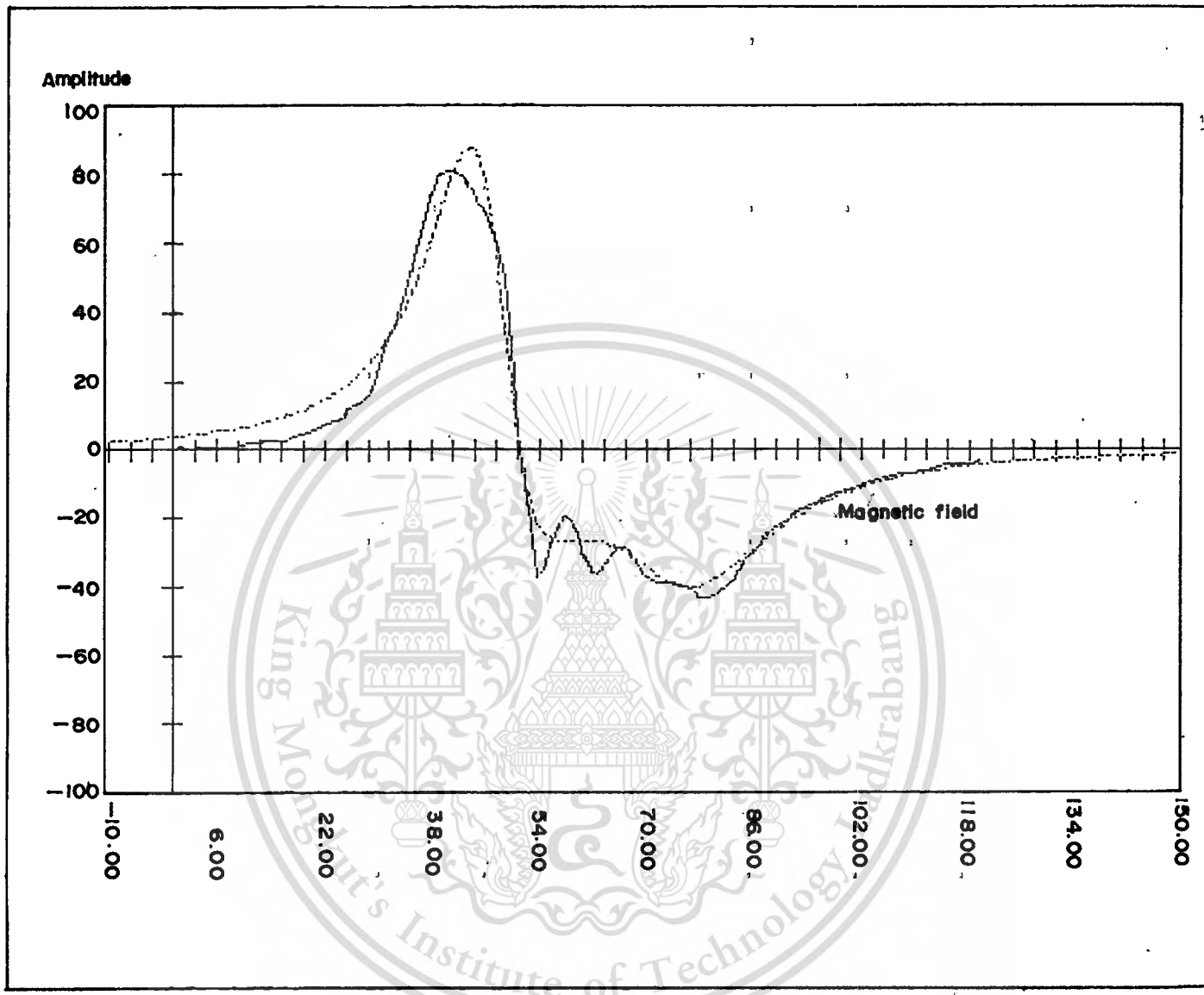

Figure 42.4 EXPERIMENTAL AND COMPUTED CURVES USING GRADIENT PROJECTION WITH 12 VARIABLES (ARBITRARY SCALE UNITS) ; —— EXPERIMENTAL CURVE, ... COMPUTED CURVE AT TEMPERATURE 84° K

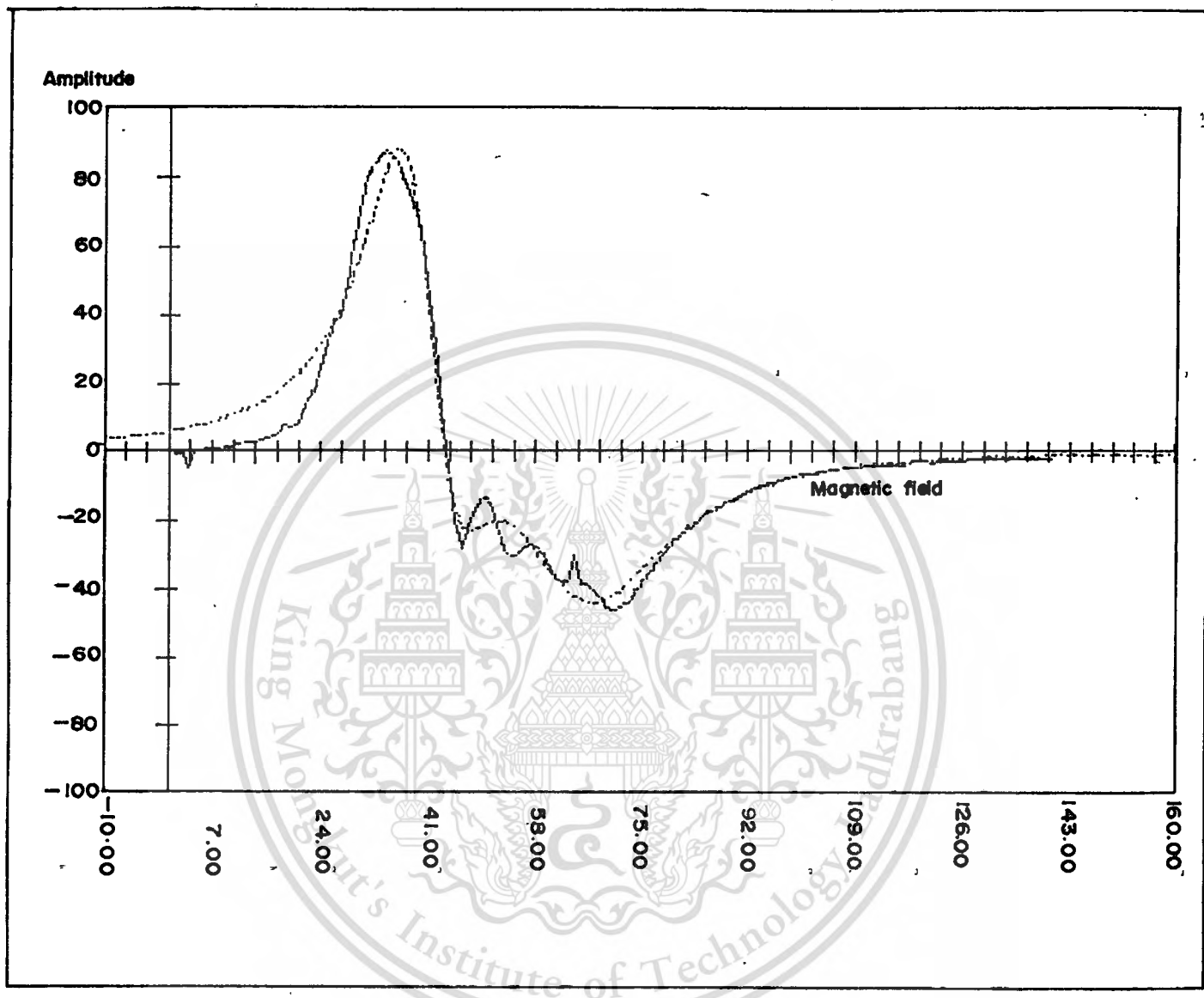

Figure 4.2.5 EXPERIMENTAL AND COMPUTED CURVES USING GRADIENT PROJECTION WITH 12 VARIABLES (ARBITRARY SCALE UNITS) ; —— EXPERIMENTAL CURVE, ... COMPUTED CURVE AT TEMPERATURE 92.2° K

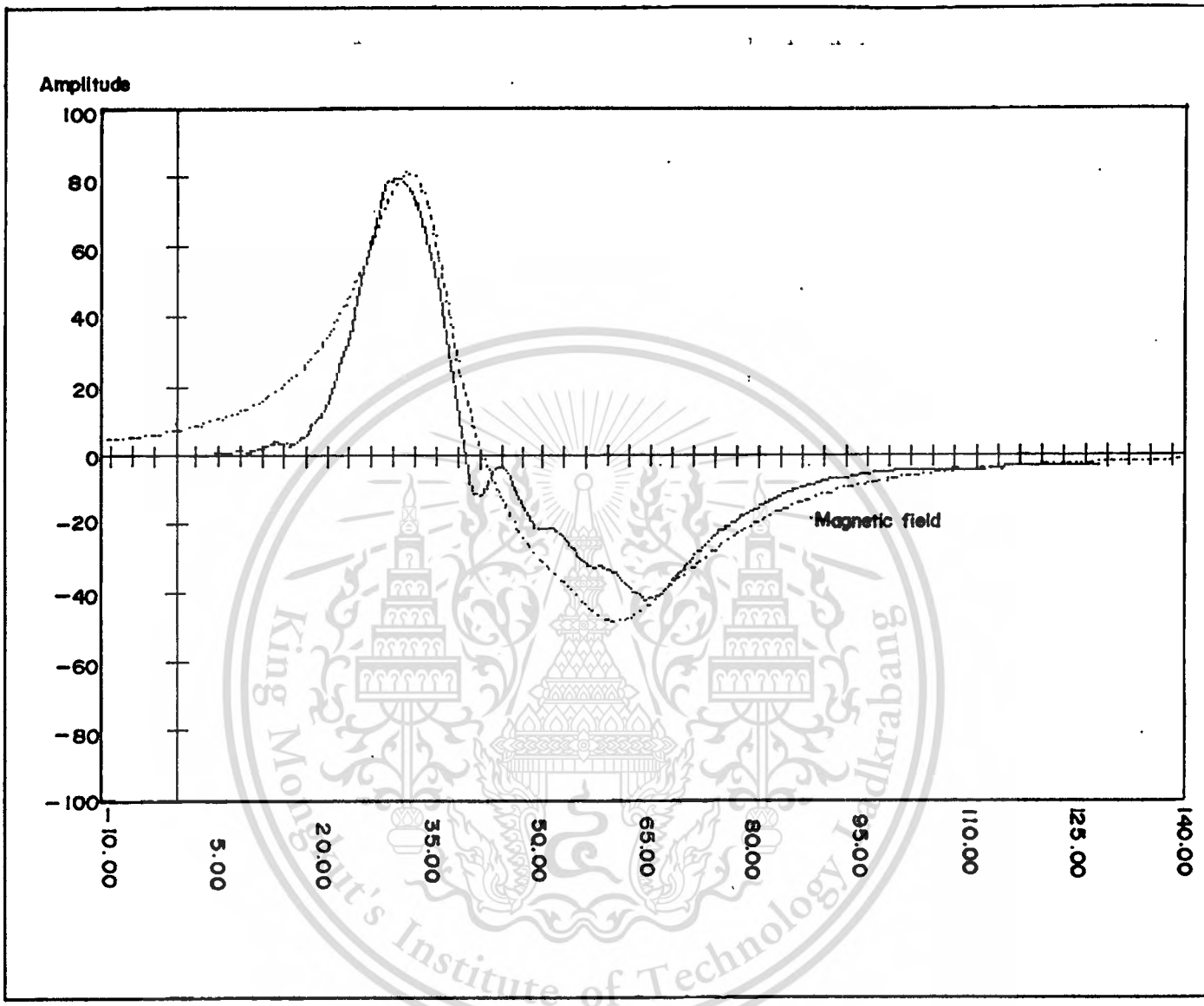

Figure 4.2.6. EXPERIMENTAL AND COMPUTED CURVES USING GRADIENT PROJECTION WITH 12 VARIABLES (ARBITRARY SCALE UNITS); —— EXPERIMENTAL CURVE, ... COMPUTED CURVE AT TEMPERATURE 102.8 K

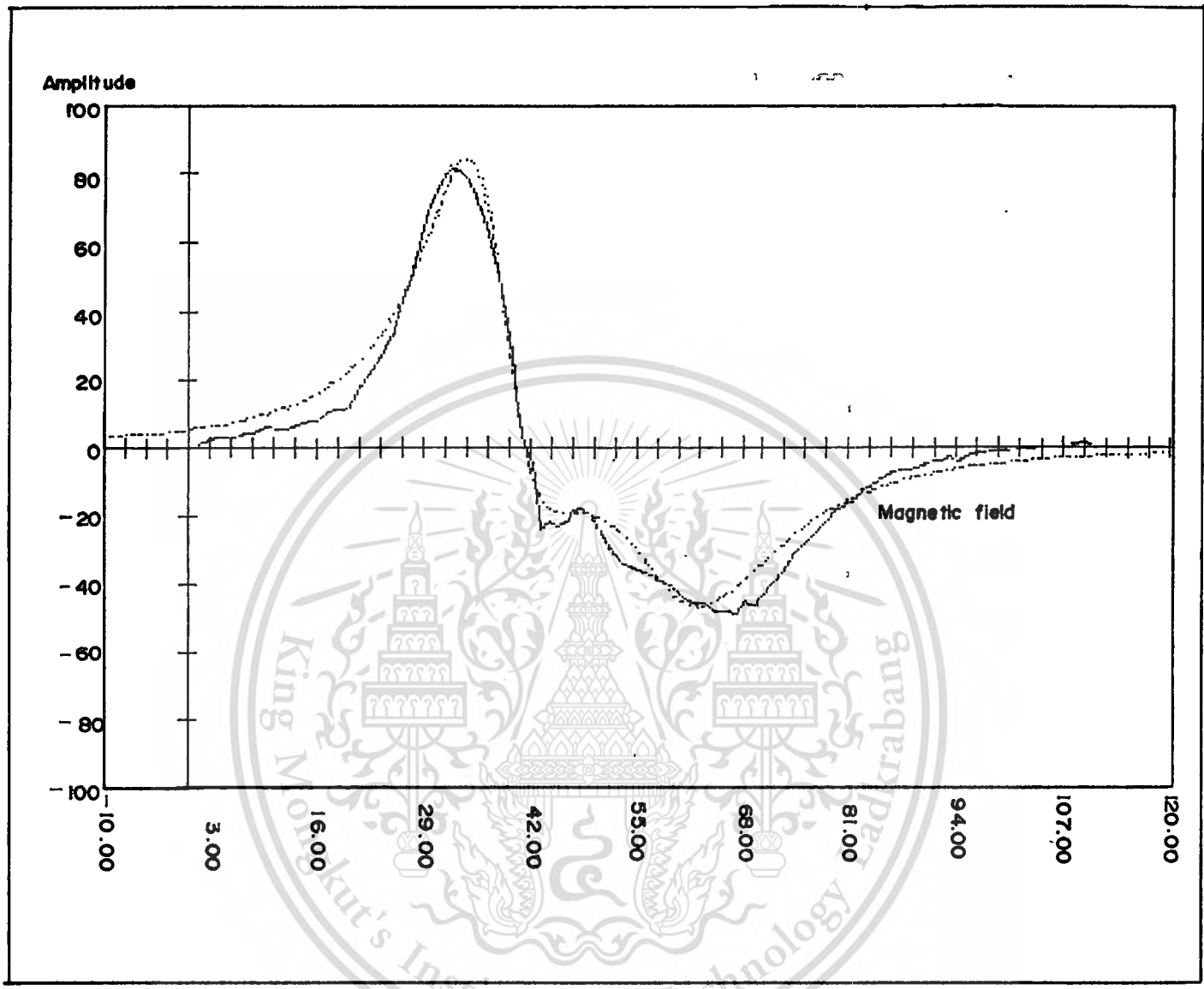

Figure 4.2.7 EXPERIMENTAL AND COMPUTED CURVES USING GRADIENT PROJECTION WITH 12 VARIABLES (ARBITRARY SCALE UNITS) ; —— EXPERIMENTAL CURVE, ... COMPUTED CURVE AT TEMPERATURE 110.4 °K

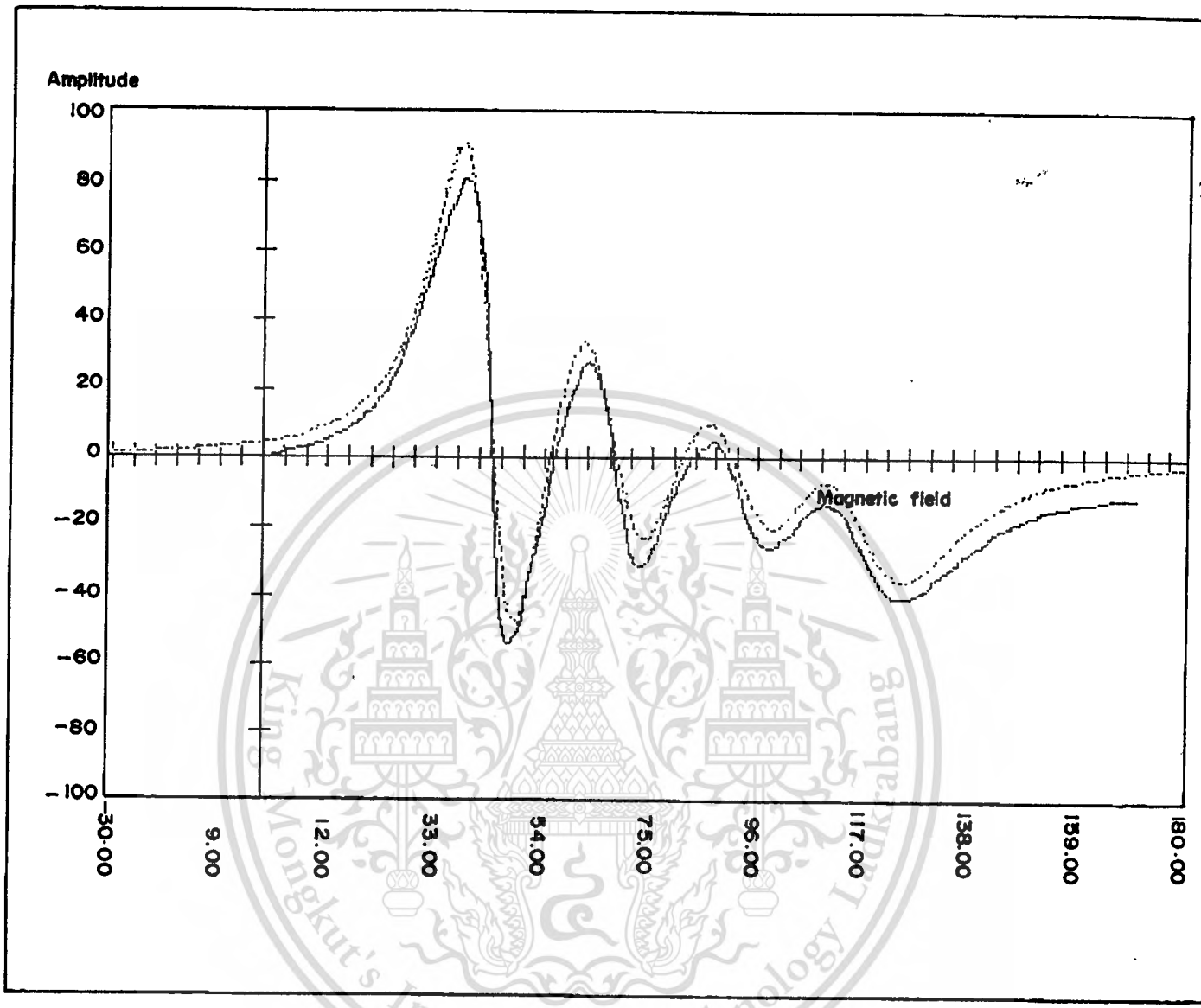

Figure 4.2.8. EXPERIMENTAL AND COMPUTED CURVES USING GRADIENT PROJECTION WITH 12 VARIABLES (ARBITRARY SCALE UNITS) ; —— EXPERIMENTAL CURVE, ... COMPUTED CURVE AT TEMPERATURE 77°K

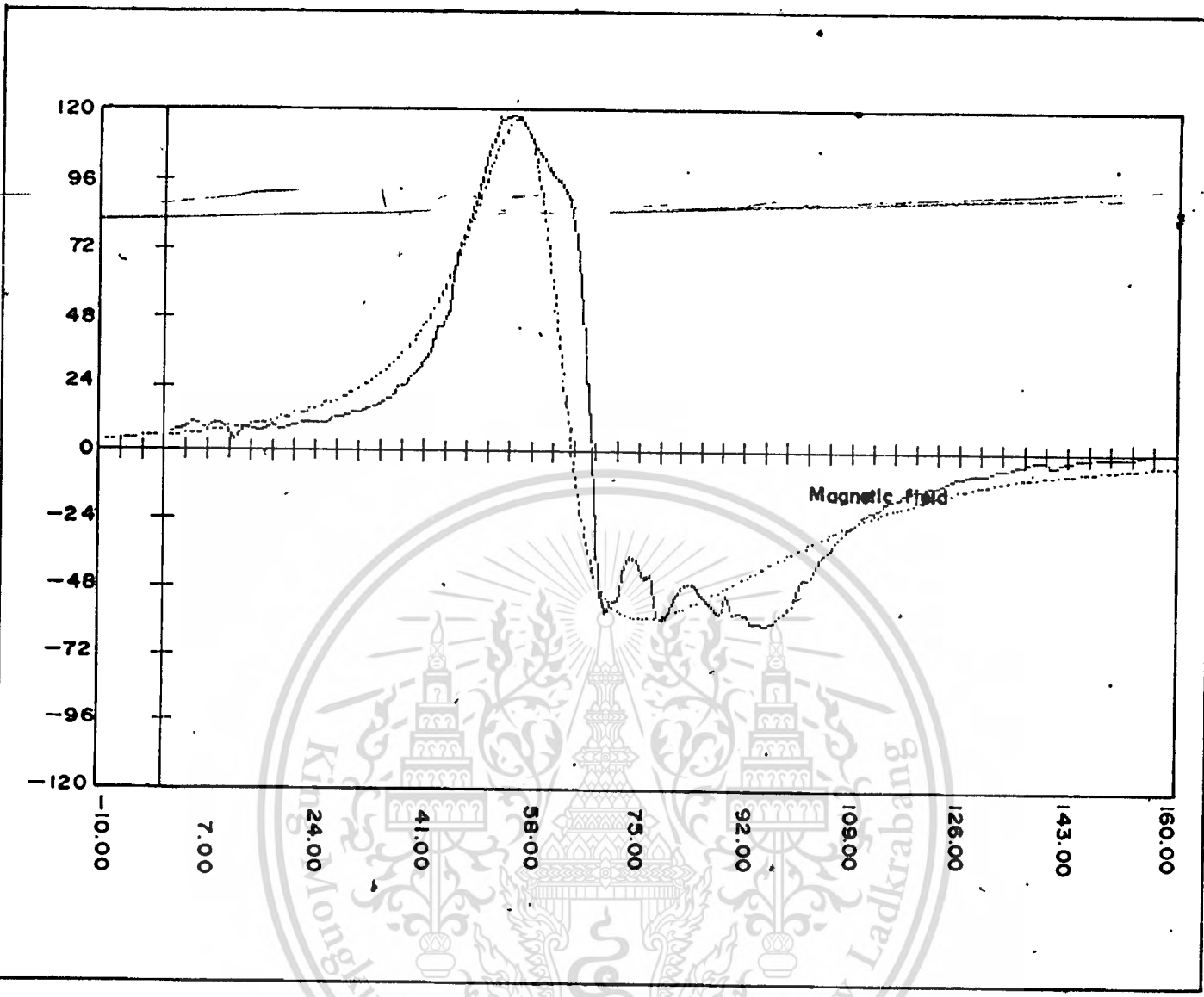

Figure 4.3.1 EXPERIMENTAL AND COMPUTED CURVES USING GAUSS NEWTON WITH 6 VARIABLES (ARBITRARY SCALE UNITS) ; —— EXPERIMENTAL CURVE, ... COMPUTED CURVE AT TEMPERATURE 76.4 K

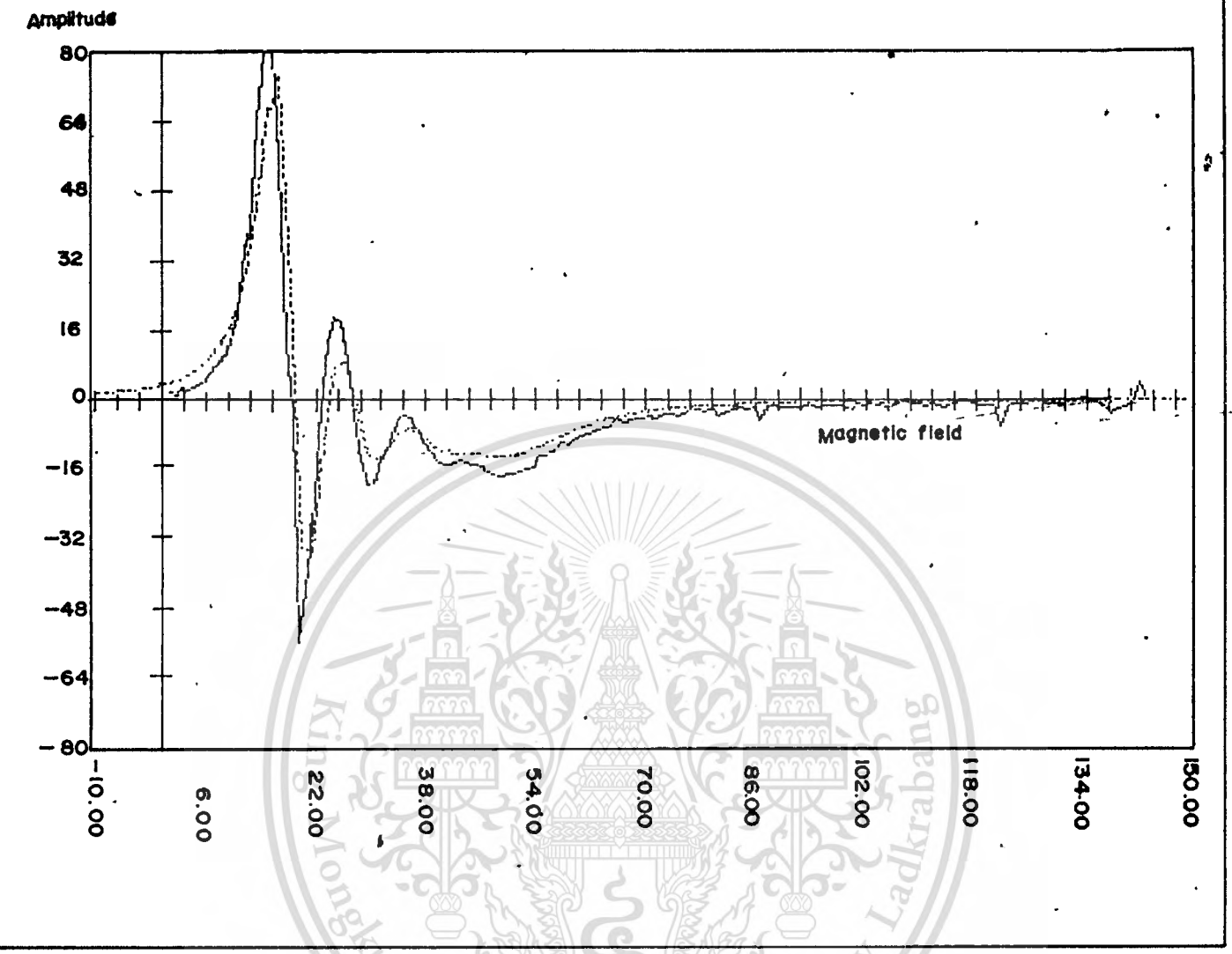

Figure4.3.2. EXPERIMENTAL AND COMPUTED CURVES USING GAUSS NEWTON WITH 3 VARIABLES (ARBITRARY SCALE UNITS); —— EXPERIMENTAL CURVE, ------ COMPUTED CURVE AT TEMPERATURE 77°K.

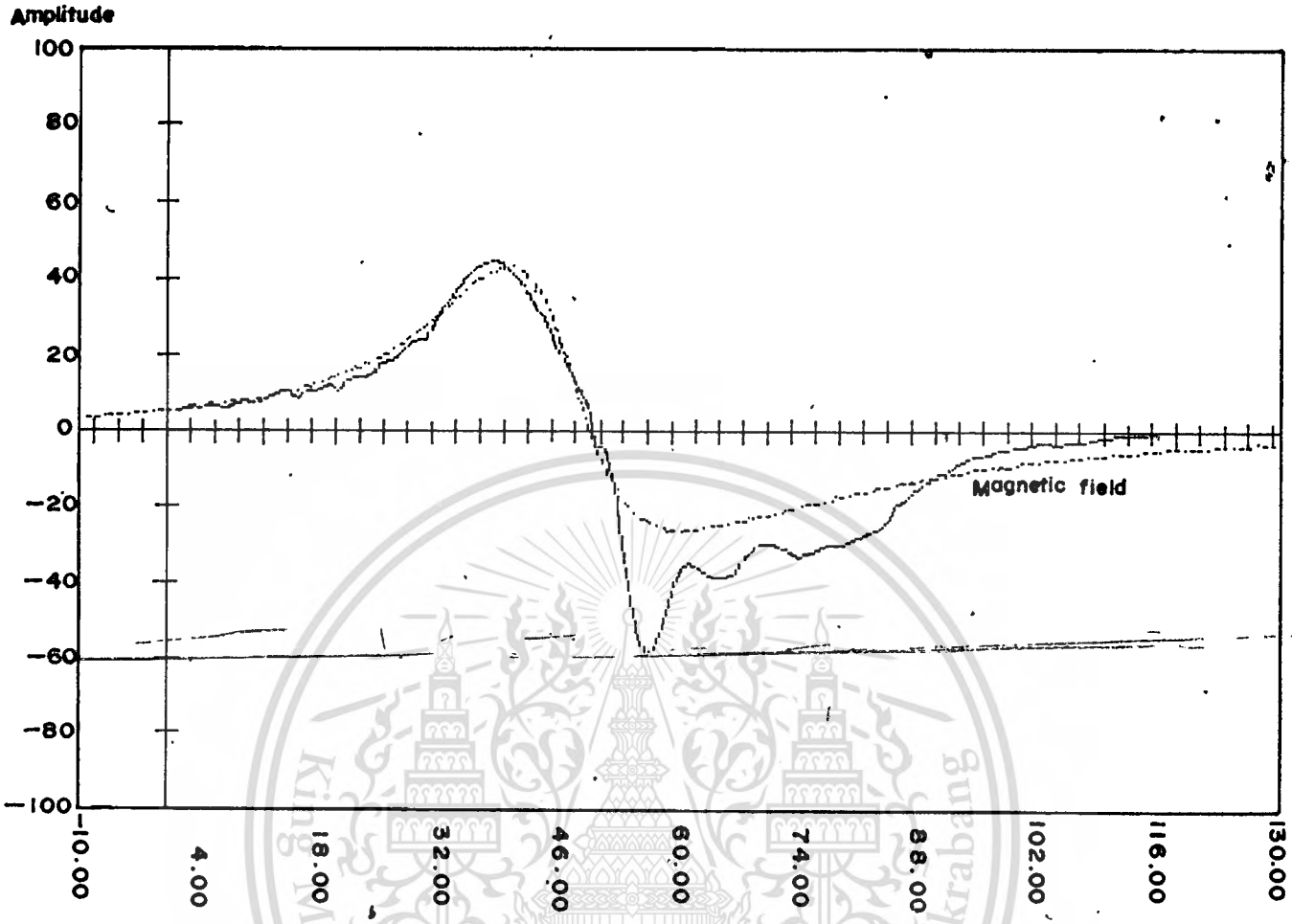

Figure 4.3.3. EXPERIMENTAL AND COMPUTED CURVES USING GAUSS NEWTON WITH 3 VARIBLES (ARBITRARY SCALE UNITS) ; —— EXPERIMENTAL CURVE, ------ COMPUTED CURVE AT TEMPERATURE 80.2 ° K

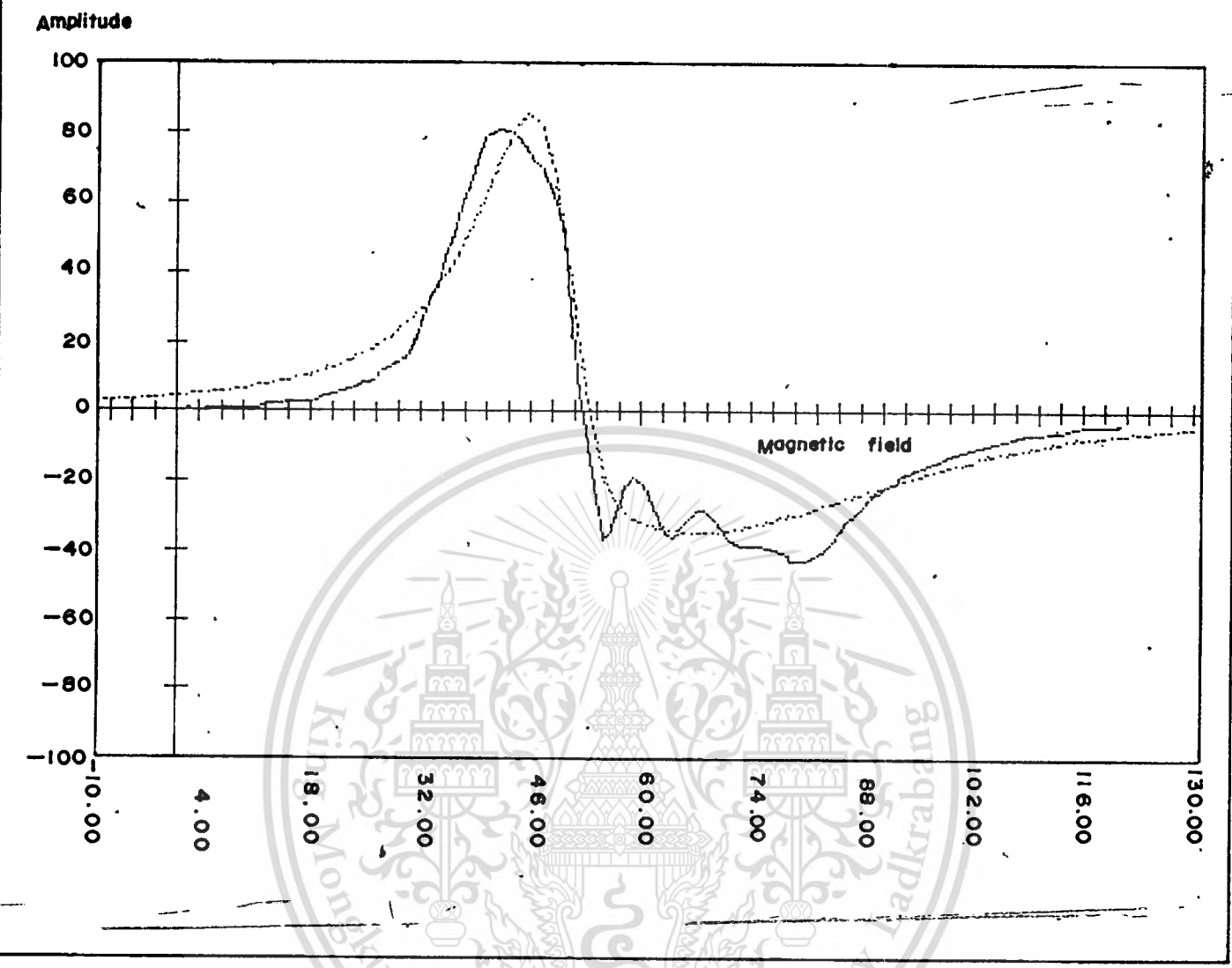

Figure 4.3.4. EXPERIMENTAL AND COMPUTED CURVES USING GAUSS NEWTON WITH 3 VARIABLES (ARBITRARY SCALE UNITS); —— EXPERIMENTAL CURVE, ... COMPUTED CURVE AT TEMPERATURE 84° K

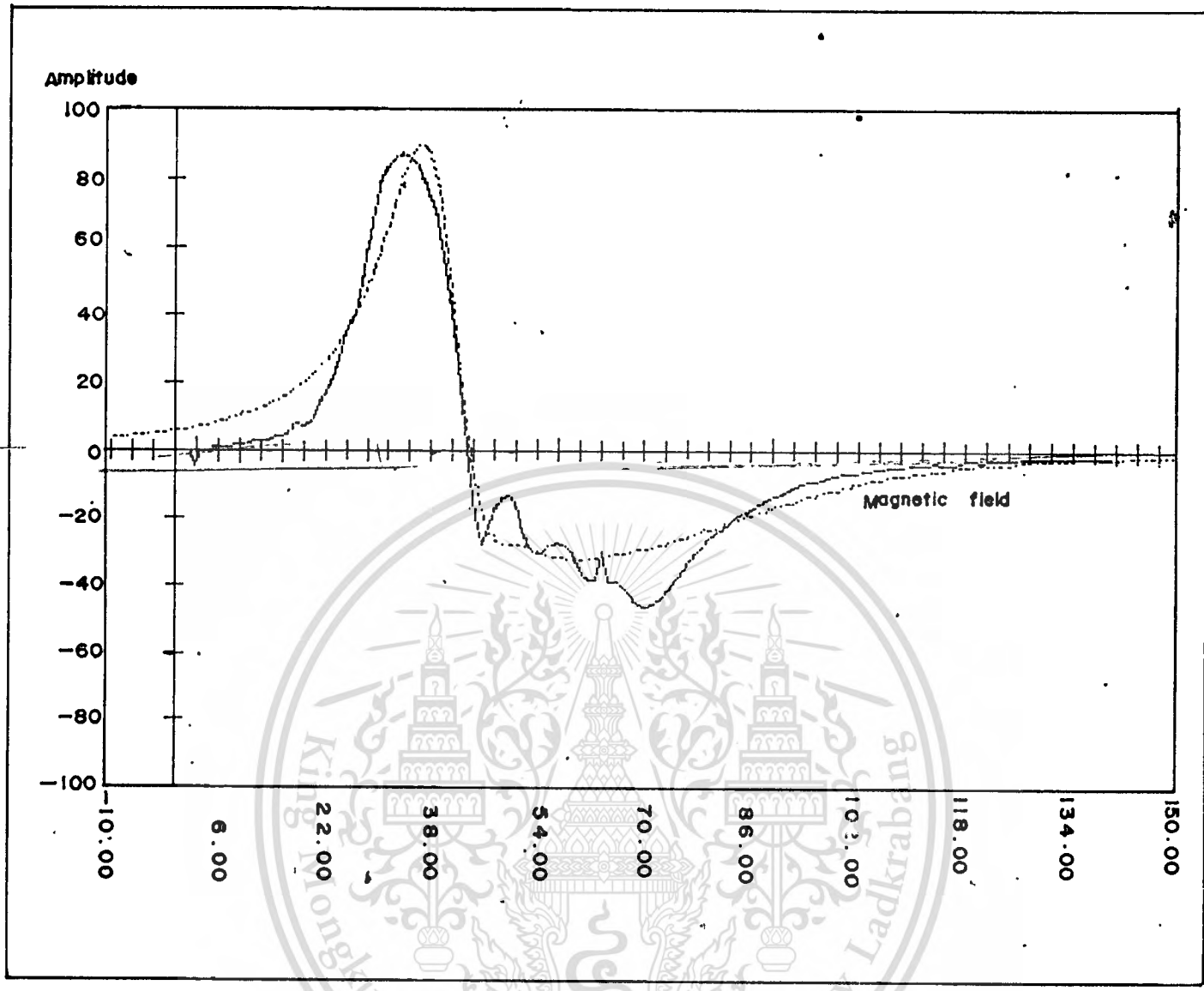

Figure 4.3.5. EXPERIMENTAL AND COMPUTED CURVES USING GUASS NEWTON WITH 3 VARIABLES (ARBITRARY SCALE UNITS) ; —— EXPERIMENTAL CURVE, ... COMPUTED CURVE AT TEMPERATURE 92.2° K.

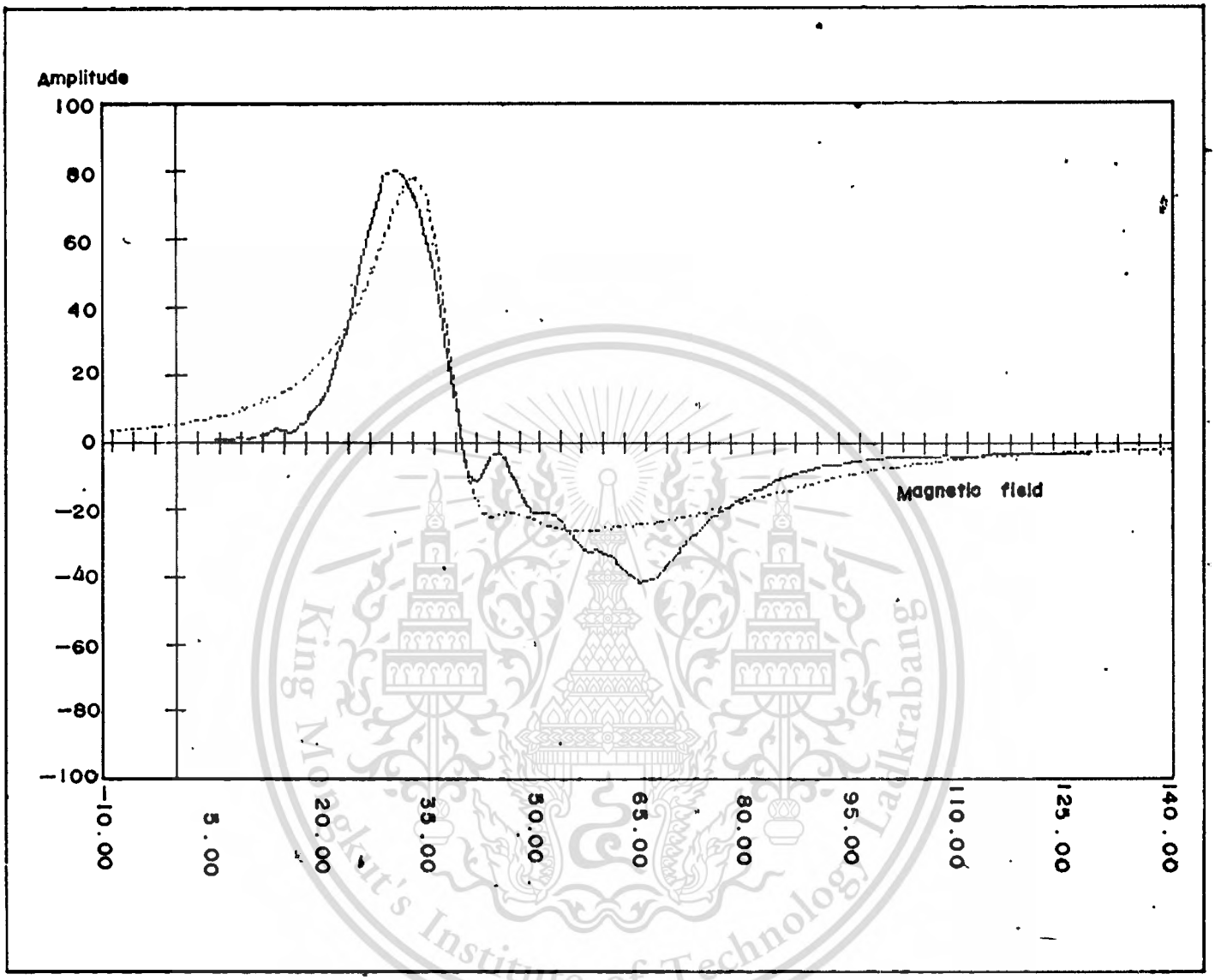

Figure 4.3.6. EXPERIMENTAL AND COMPUTED CURVES USING GAUSS NEWTON WITH 3 VARIABLES (ARBITRARY SCALE UNITS); —— EXPERIMENTAL CURVE, ····· COMPUTE CURVE AT TEMPERATUEE 102.8 ° K.

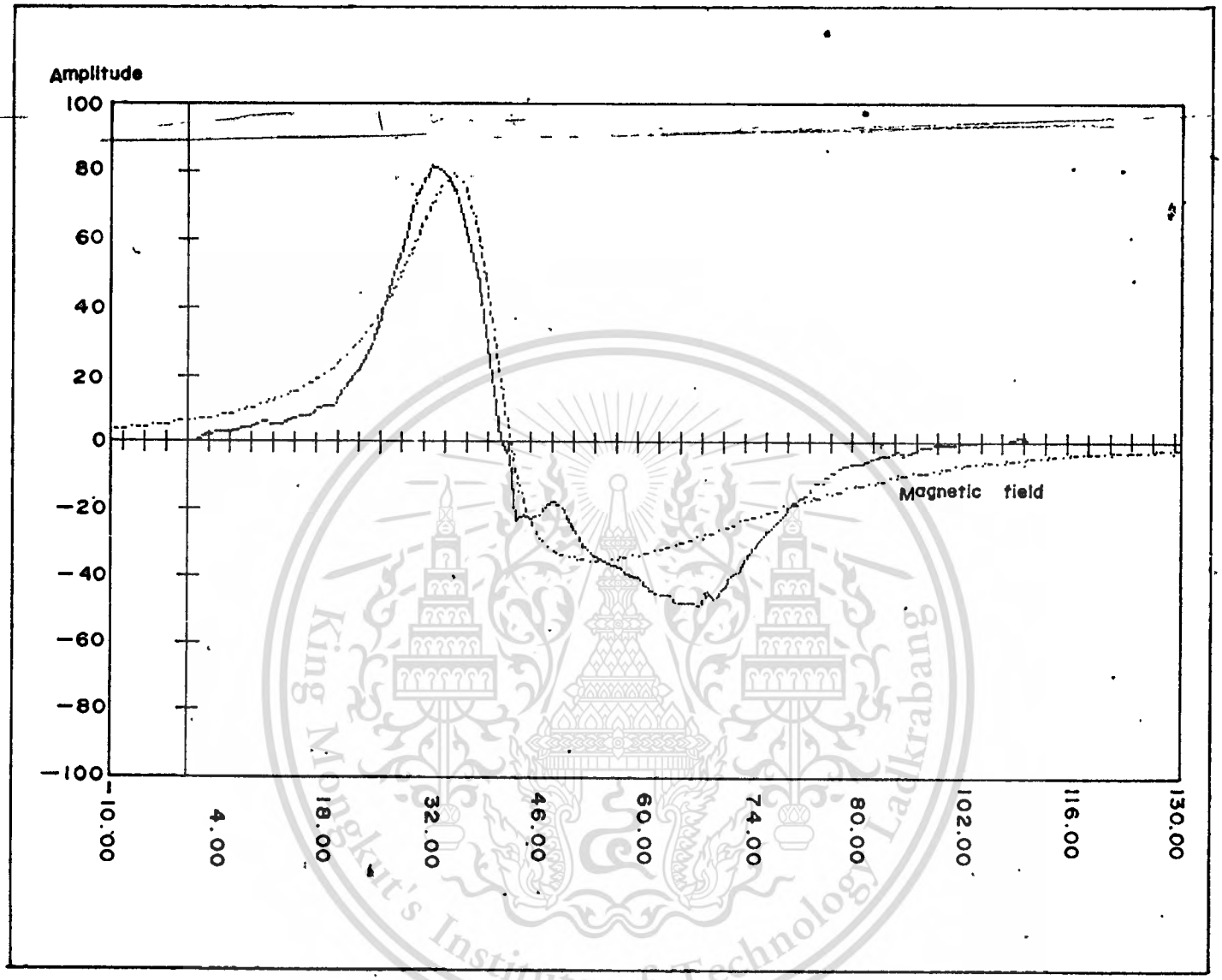

Figure 4.3.7. EXPERIMENTAL AND COMPUTED CURVES USING GAUSS NEWTON WITH 3 VARIABLES (ARBITRARY SCALE UNITS) ; —— EXPERIMENTAL CURVE, ---- COMPUTED CURVE AT TEMPERATURE 110.4° K

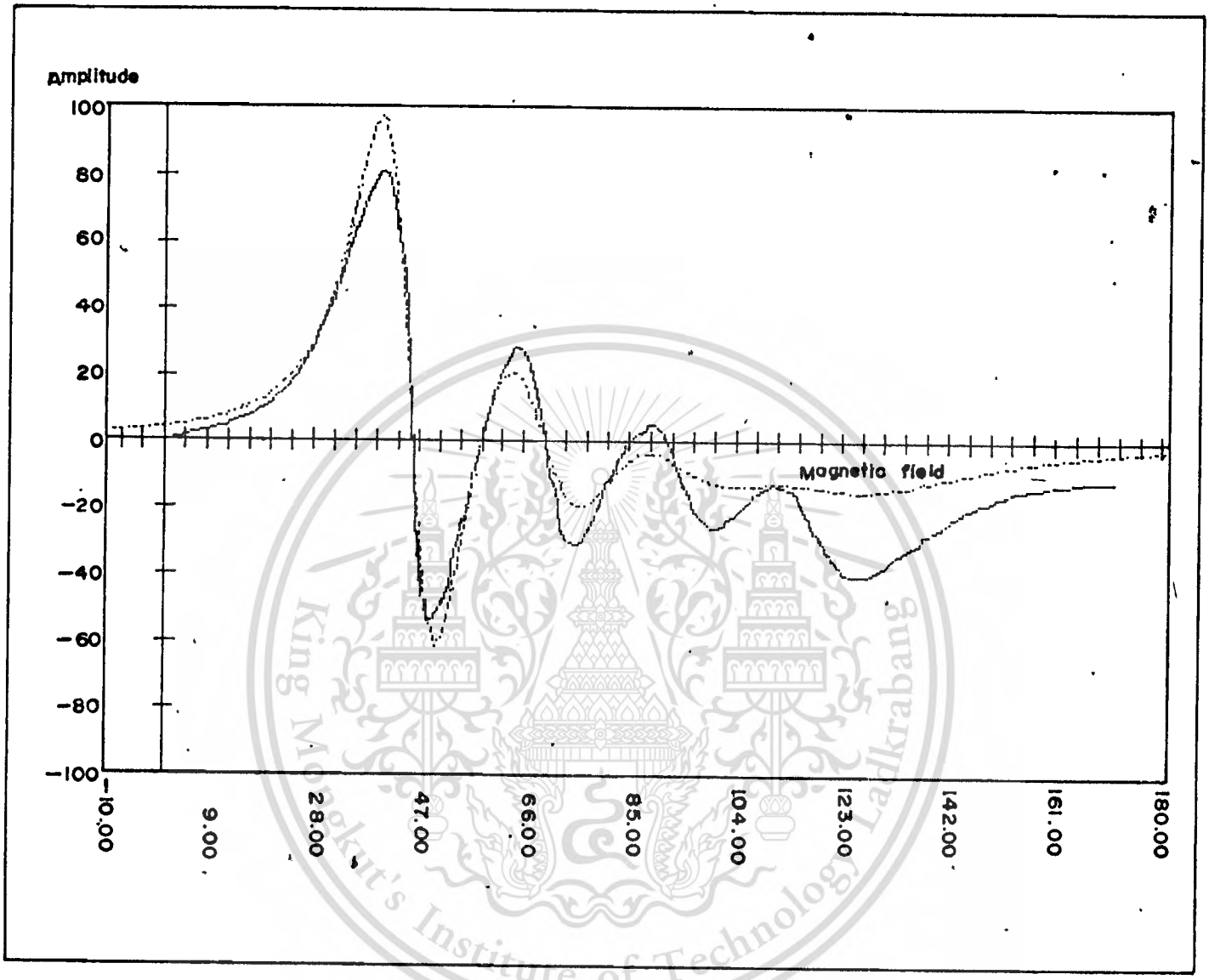

Figure 4.3.6. EXPERIMENTAL AND COMPUTED CURVES USING GAUSS NEWTON WITH 3 VARIABLES (ARBITRARY SCALE UNITS) ; —— EXPERIMENTAL CURVE, ... COMPUTED CURVE AT TEMPERATURE 77° K.

PART 5
DISCUSSION.

5.1 Method of Calculation.

In the analysis, the Gauss-Newton and the Gradient Projection are used to minimize a function of several variables. The Gauss-Newton method uses a few minutes if a good starting estimate of the unknowns is available, but takes a long time if we take a bad starting estimate. In this thesis 10-30 minutes for a good starting estimate were required, while for a bad starting estimate about 10-15 hours were required. Another method is the Gradient Projection method. The advantage of the Gradient Projection method over the Gauss-Newton method is its flexibility of initial conditions in the admissible region. So the starting point in iteration could be chosen arbitrary (as long as it occurs in the fleasible region) ,because this method will always converge to a local minimum point.

The calculation may be carried out in different ways depending on how many variables we allow. We see that if the line width of the four Lorentzian functions are made to satisfy the theoretical. Ratio of the line width according to the equation (3.3.1). With the Gauss-Newton method, we vary the remaining variables amplitude A , line width a and centre of curve ΔH . This procedure we called "calculation with 3 variables" If we allow a_1, a_2, a_3 and a_4 to vary, we see that the objective function is decreased. This we called "calculation with 6 variables". Both methods were used for this case. For the best fit function, the Gradient Projection is used allowing all the quantities, ie the 12 variables $A_1, A_2, A_3, A_4, a_1, a_2, a_3, a_4, H_{01}, H_{02}, H_{03}$ and H_{04} to vary . We see that the objective function is less than case 2 . While the Gauss-Newton and Gradient Projection methods both lead to the same solution we see that the latter has the advantage of always converging to a minimum and so is far more economical of time than the former. In the case where the number of variables becomes large, in our case 3 , calculation by the Gradient Projection is still fast,while the use of the Gauss Newton proved impossible in any reasonable length of computing time.

The success of the fitting procedure may be assessed by an examination of Fig 4.1.1-4.1.8,Fig 4.2.1-4.2.8 and Fig 4.3.1-4.3.8. The fit at 77° K is the most satisfactory and it is interesting to compare the fit for the case of computation with 6 and 12 variables Fig4.1.2,4.2.2 and Fig 4.3.2 . At this temperature the resolution of the spectrum into its four component parts is clearest. As temperature increase, the line width broaden until all four finally coalesce into a single line. In this range it was found impossible to use the Gauss-Newton method at all while the Gradient Projection continued to give a result. Inspection shows that the fit is less good than the 77° K case but is still resonable enoungh to allow physical conclutions to be made.

5.2. Physical significance of results.

5.2.1 Line shape.

The results can next be judged for their physical significance. First it has been shown that the spectrum is indeed composed of four individual lines howing a Lorentzian shape. According to theory the lines should have a) equal amplitude factor A

b) equal seperation ΔH

c) line width which vary according to the theoretical expression $\{(g_{\parallel}-g_{\perp})\beta H+(A_{\parallel}-A_{\perp})m\}^2$

The accuracy of these predictions can be judged from the results for calculation with 12 variables where the amplitude factors of individual lines, their seperation and their width are all allowed to vary. Thus if the theory is correct the amplitude factors of each line should be equal, as well as the field seperations. The results are presented for inspection in table 4.1.1,4.2.1,4.3.1 . In studying the physical significance of the analysis it may be more meaningful to restrict the amplitude factors and the field seperation to a single value (6 variables calculation) . Finally we can see how well the results can be analysed by forcing then to follow strictly the theoretical expression such that the line widths also vary as 1:1.59:2.33:3.16 (from equation 3.3.1 substituting known values of the variables) . All three cases are written in table 5.2.1.In the results for calculation with 12 variables and 6

variables, the ratio of linewidth does not follow the theoretical expression but it has an objective function less than first case. It is seen that calculation with 12 variables and 6 variables give ratio of linewidth agree closely. By inspection Fig 4.2.1-4.2.8 which are calculated with 12 variables fit better than Fig 4.1.1-4.1.8 which are calculated with 6 variables and Fig 4.3 1-4.3.8 which are calculated with 3 variables.

5.2.2 Relaxation time

The effect of the rest of the crystal on the copper ion causes transitions between the energy levels with some characteristic relaxation time T . $1/T$ increases with temperature. In section 2.3. it was shown that transformation from arbitrary units can be made to give frequency units. Using equation (2.3.7) a calculation of slope and relaxation time is shown in table 5.2.2 . We can see that the relaxation times are of order 10^{-12} .We know that at low temperature, four lines of Lorentzian shape are seperate. Each line width being seperated can be measured easily. In this range $1/T$ varies with T^5 (16). Fig 5.2.2 shows that at low temperature if we plot temperature T againt $1/T$ $1/T = 8.2\ T^5$ in the range $T > 45^{\circ}$ K . We have plotted our results on a graph showing the low temperature points and it is seen that our values are an order of magnitude greater than would be predicted by extrapolation of the low temperature line.

5.3 Conclusion.

In this thesis we have analysed the overlapping lines of a Jahn-Teller modified spectrum. The analysis has been successful in its mathematical aspects, that is the Gradient Projection Method has found to be a very suitable method of analysis for such a spectrum especially when all possible variables of the objective function are allowed to vary independently.

Considering next the physical aspect of the problem. Some success is achieved. The fact that the spectrum is fit to an objective function of four Lorentzian line shapes of varying widths follows theoretical prediction. However the expected ratio of the line

widths;Table 5.2.2, column 2 and 3 , do not follow closely the theoretical values , column 1 . Finally the derived relaxation times are also seen to deviate by about a factor of ten from values that would correlate with values measured at lower temperatures.

Two comments can be made. First the relaxation times are derived on the supposition that the line widths of the lines follow theory. Thus,a deviation in line width measurement from theory as mentioned in the last paragraph will also lead to deviation in relaxation time. Secondly, with regard the line width deviation, examination of the curve fitting shows that while in some case (e.g. Fig 4.3.2)the fit is good, in other (e.g. Fig 4.3.3) the theoretical expression clearly does not follow the variations in the overall line shape that show the effect of the individual lines.

The ultimate cause of disagreement between our values of line width and the theoretically predicted values must await a further appraisal of theory. A likely cause of disagreement is that higher energy levels of the atoms become populated at higher temerature. Such atoms would give a different spectrum so that the observed spectrum would be the superposition of two spectra leading to erroneous results when it is analysed as a single spectrum. At 77° K (Fig 4.3.2,4.2.2,and 4.1.2) where the analysed line widths are closest to theory the spectrum is seen to consist clearly of a single set of four lines. But at 92.2° K inspection of the experimental curve shows evidence of an overlapping wider spectrum and one with norrower components. Further clarification cannot be made within the scope of this thesis. But indication have been offered of where further investigation may be fruitful.

Table 5.2.1 The results of line width in 3 cases.

	Calculation with 3 variables	Calculation with 6 variables	Calculation with 12 variables
1	1:1.59:2.33:3.16	1:0.83:1.59:1.27	1:0.81:1.40:1.29
2	1:1.59:2.33:3.16	1:1.33:1.85:2.47	1:1.27:2.10:2.73
3	1:1.59:2.33:3.16	1:1.14:1.88:1.94	1:0.63:1.23:1.37
4	1:1.59:2.33:3.16	1:1.63:2.28:1.78	1:1.62:2.31:1.83
5	1:1.59:2.33:3.16	1:2.09:1.94:1.88	1:2.00:1.86:1.87
6	1:1.59:2.33:3.16	1:1.85:1.65:1.89	1:0.73:1.04:1.87
7	1:1.59:2.33:3.16	1:1.78:1.90:1.50	1:1.72:1.93:1.65
	average	average	average
	1:1.59:2.33:3.16	$1:1.52\pm0.44$:1.87 ± 0.22:1.82 ± 0.38	$1:1.25\pm0.54$:1.70 ± 0.48:1.802 ± 0.47
8	1:1.37:1.79:2.28	1:1.28:1.53:1.76	1:1.38:1.68:1.77

1.at 76.4° K
2 at 77.0° K
3 at 80.2° K
4 at 84.0° K
5 at 92.2° K
6 at 102.8° K
7 at 110.4° K
8 at 77.0° K

Table 5.2.2 Relaxation time.

Temperature K	T (calculation)	T (theoretical)
76	4.094×10^{-12}	46.8×10^{-12}
77.0	9.091×10^{-12}	45.0×10^{-12}
80.2	2.531×10^{-11}	3.68×10^{-11}
84.0	1.125×10^{-11}	2.90×10^{-11}
92.2	8.617×10^{-12}	18.0×10^{-12}
102.8	7.386×10^{-12}	10.6×10^{-12}
110.4	4.212×10^{-12}	7.4×10^{-12}
77.0	6.318×10^{-12}	18.25×10^{-12}

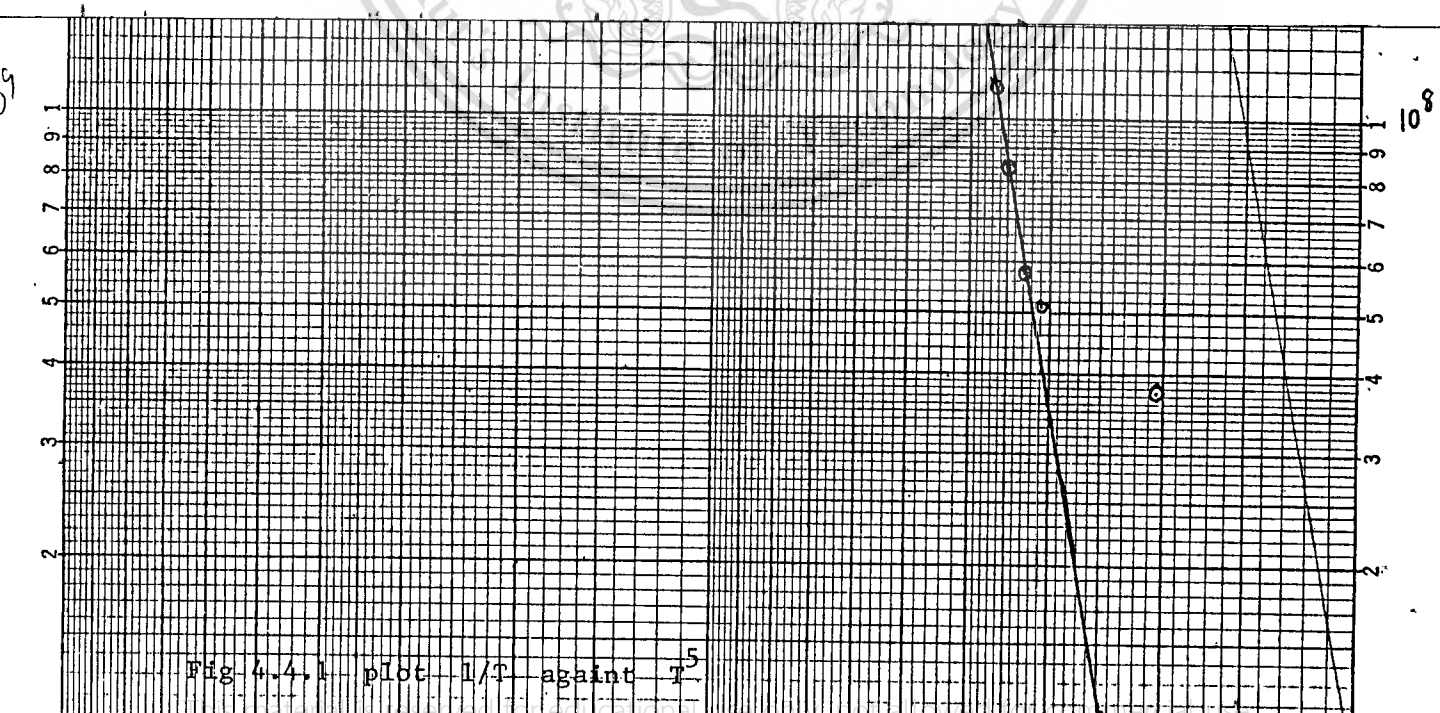

Fig 4.4.1 plot 1/T against T^5

PART 6
CONCLUSION

PART 2 presents the theoretical background of the Jahn-Teller Theory. It was shown the spectral line shape and spin Hamiltonian.

PART 3 presents the Jahn-Teller Theory. The Cu^{2+} in octahedral field and electron paramagnetic spectrum.

PART 4 presents method of analysis and results, which can be used to fixed theoretical curve to a experimental curve.

section 4.1 presents a method of Gauss-Newton which expanded the function with Tayler's series. This method has proved effective where good starting estimates of the unknown are available.

section 4.2 presents a method of Gradient Projection. There is good feature for this method, one can introduce a constraint for each parameter. So, starting point in iteration could be chosen arbitraly (as long as it belongs to feasible region), because this algorithm will alway converge to local minimum point. It was shown that the agreement of Gauss-Newton and Gradient Projection method.

section 4.3 Shows a results which calculate from Gradient Projection with 12 variations and Gauss-Newton 6 and 3 variables and determine a relaxation time.

PART 5 Discussion.

PART 7
APPENDIX

GRADIENT PROJECTION WITH 12 VARIATIONS

```
10    INPUT "# OF VARIABLE",N1
20    INPUT "# OF IN. EQ. CONSTRAINT",N2
30    INPUT "# OF DATA",Kk
40    CALL Sss(N1,N2,Kk)
50    SUB Sss(N1,N2,Kk)
60    OPTION BASE 1
70        SHORT N1(N1,N2),B(N2),Y(N1),A1(N2,N1),A2(N2),A3(N2),A4(N1,N2),Rr(N2),A
N2,N1),A6(N2,N2),A7(N2,N2),A8(N1,N1),A9(N2,N1),B1(N1,N1),Pq(N1,N1),Fy(N1)
80        SHORT B2(N1),B3(N2),B4(N2),B5(N1),Tt(N2),B6(N1),B8,Kk1,C1(N1),C4,Ff(N1
Yy(N1),A44(N1,N2),Rrr(N2),A77(N2,N2),Rv(N2),Y99(N1),Dd(Kk),X(Kk)
90    INPUT "TOL 1",E1
100   INPUT "TOL 2",E2
110   Wr0=1
120   Wr=.1
130   FOR I=1 TO N1
140   N1(I,I)=1
150   N1(I,I+N1)=-1
160   NEXT I
170   FOR I=1 TO 4
180   B(I)=5600
190   B(I+N1)=-5700
200   NEXT I
210   FOR I=5 TO 8
220   B(I)=8
230   B(I+N1)=-20
240   NEXT I
250   FOR I=9 TO 12
260   B(I)=60
270   B(I+N1)=-90
280   NEXT I
290   ASSIGN #1 TO "DATAE2:T14"
300   READ #1,1;Dd(*),X(*)
310   FOR I=1 TO N1
320   DISP " Y(";I;")";
330   INPUT Y(I)
340   NEXT I
350   PRINT "MAT NL";N1(*),"MAT-B";B(*),"MAT-Y0";Y(*)
360   MAT A1=TRN(N1)
370   MAT A2=A1*Y
380   MAT A3=A2-B
390   MAT Rr=ZER(N2)
400   K=0
410   FOR I=1 TO N2
420   S99=A3(I)
430   IF ABS(S99)<>0 THEN 490
440   K=K+1
450   FOR J=1 TO N1
460   A4(J,K)=N1(J,I)
470   Rr(K)=I
480   NEXT J
490   NEXT I
500   Ite=-1
510 Loop: !
```

```
520  Wr0=1
530  Wr=.1
540  M79=0
550  Ite=Ite+1
560  PRINT "ITE=";Ite
570  Rq=0
580  Bq=0
590  IF K<>0 THEN 630
600  MAT Rr=ZER(N2)
610  MAT Pq=IDN(N1,N1)
620  GOTO 770
630   REDIM A44(N1,K),A5(K,N1),A6(K,K),A7(K,K),A9(K,N1),B3(K),B4(K)
640   FOR I=1 TO N1
650   FOR J=1 TO K
660   A44(I,J)=A4(I,J)
670   NEXT J
680   NEXT I
690  MAT A5=TRN(A44)
700  MAT A6=A5*A44
710  MAT A7=INV(A6)
720 Box1: !
730  MAT A8=IDN(N1,N1)
740  MAT A9=A7*A5
750  MAT B1=A44*A9
760  MAT Pq=A8-B1
770  GOSUB Dfy!
780  PRINT "MAT-Y";Y(*)
790  PRINT "OBJECTIVE FUNCTION=";Mmm
800  MAT Ff=Fy
810  MAT B2=Pq*Fy
820  S1=0
830  FOR I=1 TO N1
840  S1=S1+B2(I)^2
850  NEXT I
860  S1=SQR(S1)
870  IF K<>0 THEN 890
880  GOTO 960
890  MAT B3=A9*Fy
900  Rq=-1E99
910  FOR I=1 TO K
920  IF Rq>B3(I) THEN 950
930  Rq=B3(I)
940  T1=I
950  NEXT I
960  IF K=N1 THEN Trq!
970  IF S1<=E1 THEN Trq !
980  IF K<>0 THEN 1000
990  GOTO 1600
1000 MAT A77=ABS(A7)
1010 MAT B4=RSUM(A77)
1020 Bq=-1E99
```

```
1030 FOR I=1 TO K
1040 IF Bq>B4(I) THEN 1060
1050 Bq=B4(I)
1060 NEXT I
1070 IF Rq>Bq THEN Dh!
1080 GOTO Box3  !
1090 Trq:!
1100 IF K<>0 THEN 1120
1110 GOTO 1130
1120 IF Rq>0 THEN Dh!
1130 PRINT "PROGRAM STOP ;SATISFY"
1140 PRINT "SOLUTION";Y(*)
1150 PRINT "OBJECTIVE FUNCTION =";Mmm
1160 GOTO 310
1170 STOP
1180 Dh:!
1190 PRINT "DROP PLANE #",Rr(T1)
1200 IF K<>1 THEN 1240
1210 K1=0
1220 MAT Pq=IDN(N1,N1)
1230 GOTO 1520
1240 FOR J=1 TO K
1250 IF J=T1 THEN 1310
1260 FOR I=1 TO N1
1270 A4(I,J)=A4(I,J)
1280 Rv(J)=Rr(J)
1290 NEXT I
1300 NEXT J
1310 FOR I=1 TO N1
1320 FOR Jj=J TO K-1
1330 A4(I,Jj)=A4(I,Jj+1)
1340 Rv(Jj)=Rr(Jj+1)
1350 NEXT Jj
1360 NEXT I
1370 K1=K-1
1380 REDIM A44(N1,K1),A5(K1,N1),A6(K1,K1),A7(K1,K1),A9(K1,N1),B5(N1)
1390 FOR I=1 TO N1
1400 FOR J=1 TO K1
1410 A44(I,J)=A4(I,J)
1420 NEXT J
1430 NEXT I
1440 REDIM A4(N1,K1)
1450 MAT A4=A44
1460 MAT A5=TRN(A44)
1470 MAT A6=A5*A44
1480 MAT A7=INV(A6)
1490 MAT A9=A7*A5
1500 MAT B1=A44*A9
1510 MAT Pq=A8-B1
1520 M79=1
1530 MAT B2=Pq*Fy
```

```
1540 S1=0
1550 FOR I=1 TO N1
1560 S1=B2(I)^2+S1
1570 NEXT I
1580 S1=SQR(S1)
1590 Box3:!
1600 S2=1/S1
1610 MAT B5=(S2)*B2
1620  IF K=0 THEN 1840
1630   S4=0
1640   MAT Rrr=ZER(N2)
1650   FOR I=1 TO N2
1660   FOR J=1 TO K
1670   IF I<>Rr(J) THEN 1690
1680   GOTO 1820
1690   NEXT J
1700   S4=S4+1
1710   Rrr(S4)=I
1720   S2=0
1730   S3=0
1740   FOR L=1 TO N1
1750   S2=S2+N1(L,I)*Y(L)
1760   S3=S3+N1(L,I)*B5(L)
1770   NEXT L
1780   IF S3<>0 THEN 1810
1790   Tt(I)=-1E9
1800   GOTO 1820
1810   Tt(S4)=(B(I)-S2)/S3
1820   NEXT I
1830   GOTO 1960
1840   FOR I=1 TO N2
1850   S2=0
1860   S3=0
1870   FOR L=1 TO N1
1880   S2=S2+N1(L,I)*Y(L)
1890   S3=S3+N1(L,I)*B5(L)
1900   NEXT L
1910   IF S3<>0 THEN 1940
1920   Tt(I)=-1E9
1930   GOTO 1950
1940   Tt(I)=(B(I)-S2)/S3
1950   NEXT I
1960 Ttq=1E99
1970 Ad=0
1980 FOR I=1 TO N2-K
1990 IF Tt(I)<=0 THEN 2060
2000 IF Tt(I)>Ttq THEN 2060
2010 Ttq=Tt(I)
2020   IF K<>0 THEN 2050
2030   Ad=I
2040   GOTO 2060
```

```
2040   GOTO 2060
2050 Ad=Rrr(I)
2060 NEXT I
2070 IF Ad<>0 THEN 2100
2080 PRINT "ALL PLANE IS IMPOSSIBLE TO REACH (Tm ARE <or = 0)"
2090 STOP
2100 MAT B6=(Ttq)*B5
2110 MAT Yy=Y+B6
2120 MAT Y99=Y
2130 MAT Y=Yy
2140 GOSUB Dfy!
2150 B8=0
2160 FOR I=1 TO N1
2170 B8=B8+B5(I)*Fy(I)
2180 NEXT I
2190 IF M79<>1 THEN 2210
2200 MAT Rr=Rv
2210 IF B8>=0 THEN Ah     !
2220 B88=ABS(B8)
2230 Kk1=0
2240 FOR I=1 TO N1
2250 Kk1=Kk1+B5(I)*Ff(I)
2260 NEXT I
2270 C88=MIN(Kk1,B88)
2280 ! Wr99=Kk1
2290 Et=0
2300 Cc1=Kk1/(Kk1-B8)
2310 MAT B6=(Ttq)*B5
2320 PRINT "KK1=",Kk1
2330 Et=Et+1
2340 MAT C1=(Cc1)*B6
2350 MAT Y=Y99+C1
2360 GOSUB Dfy!
2370 C4=0
2380 FOR I=1 TO N1
2390 C4=C4+B5(I)*Fy(I)
2400 NEXT I
2410 C44=ABS(C4)
2420   PRINT "C88=";C88
2430   PRINT "C44=";C44
2440   PRINT "CC1=";Cc1
2450   PRINT "C4=";C4
2460 IF C44<E2 THEN 2830
2470 IF Et>9 THEN 2870
2480 IF C44>=C88 THEN 2580
2490 C88=C44
2500 IF C4<0 THEN 2550
2510 Ttq=(1-Cc1)*Ttq
2520 Kk1=C4
2530 MAT Y99=Y
2540 GOTO 2300
```

```
2550 B8=C4
2560 Ttq=Ttq*Cc1
2570 GOTO 2300
2580 IF Et=1 THEN 2600
2590 GOTO 2830
2600 FOR J=0 TO Wr0 STEP Wr
2610   IF J<>0 THEN 2650
2620   Cmin=Kk1
2630   J9=0
2640   GOTO 2770
2650 MAT C1=(J)*B6
2660 MAT Y=Y99+C1
2670 GOSUB Dfy!
2680 C4=0
2690 FOR I=1 TO N1
2700 C4=C4+B5(I)*Fy(I)
2710 NEXT I
2720 C4=ABS(C4)
2730 IF C4>Cmin THEN 2780
2740 Cmin=C4
2750 MAT Yy=Y
2760   J9=J
2770 NEXT J
2780 IF J9<>0 THEN 2820
2790 Wr=Wr/10
2800 Wr0=Wr0/10
2810 GOTO 2580
2820 MAT Y=Yy
2830 IF M79<>1 THEN 2860
2840 K=K1
2850 GOTO Loop !
2860 K=K
2870 GOTO Loop !
2880 Ah:!
2890 PRINT "ADD PLANE #",Ad
2900 IF M79<>1 THEN 3060
2910 K=K1+1
2920 REDIM A44(N1,K)
2930 IF K=1 THEN 2990
2940 FOR I=1 TO N1
2950 FOR J=1 TO K1
2960 A44(I,J)=A4(I,J)
2970 NEXT J
2980 NEXT I
2990 FOR I=1 TO N1
3000 A44(I,K)=N1(I,Ad)
3010 NEXT I
3020 REDIM A4(N1,K)
3030 MAT A4=A44
3040 Rr(K)=Ad
3050 GOTO Loop !
```

```
3060 K=K+1
3070 REDIM A44(N1,K)
3080 IF K=1 THEN 3140
3090 FOR I=1 TO N1
3100 FOR J=1 TO K-1
3110 A44(I,J)=A4(I,J)
3120 NEXT J
3130 NEXT I
3140 FOR I=1 TO N1
3150 A44(I,K)=N1(I,Ad)
3160 NEXT I
3170 REDIM A4(N1,K)
3180 MAT A4=A44
3190 Rr(K)=Ad
3200 GOTO Loop !
3210 SUBEND
3220 Dfy:!
3230 Su=0
3240 FOR I=1 TO N1
3250 Fy(I)=0
3260 NEXT I
3270 FOR Ii=1 TO Kk
3280 H=Dd(Ii)
3290 Yyy=0
3300 FOR N=1 TO 4
3310 W=H-Y(N+8)
3320 Yyy=Yyy-4*Y(N)*Y(N+4)*W/(Y(N+4)^2+W^2)^2
3330 NEXT N
3340 Xii=X(Ii)-Yyy
3350 FOR N=1 TO 4
3360 W=H-Y(N+8)
3370 Fy(N)=Fy(N)-8*Xii*Y(N+4)*W/(Y(N+4)^2+W^2)^2
3380 Fy(N+4)=Fy(N+4)-8*Xii*Y(N)*W*(1/(Y(N+4)^2+W^2)^2-4*Y(N+4)^2/(Y(N+4)^2+W^2)
3)
3390 Fy(N+8)=Fy(N+8)-8*Xii*Y(N)*Y(N+4)*(-1/(Y(N+4)^2+W^2)^2+4*W^2/(Y(N+4)^2+W^2
^3)
3400 NEXT N
3410 Su=Su+Xii^2
3420 NEXT Ii
3430 Mmm=Su
3440 RETURN
3450 END
```

GAUSS-NEWTON WITH 12 VARIATIONS

```
10   OPTION BASE 1
20   DIM Dd(200),Y(200),Yy(200),Aa(200,12),A(12,200),B(12,12),C(12),D(12,12),X
12),Xxx(12),X(12)
30   PRINTER IS 16
40    INPUT "# OF VARIABLE",Nn
50   INPUT "TOLERANCE ",Aaa
60   INPUT "# OF ITERATION",Kkk
70   INPUT "# OF INPUT DATA",Kk
80   REDIM Dd(Kk),Y(Kk),Yy(Kk),Aa(Kk,Nn),A(Nn,Kk),B(Nn,Nn),C(Nn),D(Nn,Nn),Xx(Nn
,Xxx(Nn),X(Nn)
90   ASSIGN #2 TO "DATAE1 :T14"
100  READ #2,1;Dd(*),Y(*)
110  L11=0
120  FOR I=1 TO Nn
130  DISP "X(";I;")";
140  INPUT X(I)
150  NEXT I
160  PRINTER IS 16
170  PRINT X(*);"INITIAL X";LIN(3)
180  DISP "WORKING!!!!!"
190  L11=L11+1
200  IF L11>Kkk THEN 510
210  Su=0
220  FOR Ii=1 TO Kk
230  H=Dd(Ii)
240  Yyy=0
250  FOR N=1 TO 4
260  W=H-X(N+8)
270  Yyy=Yyy-4*X(N)*X(N+4)*W/(X(N+4)^2+W^2)^2
280  Aa(Ii,N)=-4*X(N+4)*W/(X(N+4)^2+W^2)^2
290  Aa(Ii,N+4)=-4*X(N)*W*(1/(X(N+4)^2+W^2)^2-4*X(N+4)^2/(X(N+4)^2+W^2)^3)
300  Aa(Ii,N+8)=-4*X(N)*X(N+4)*(-1/(X(N+4)^2+W^2)^2+4*W^2/(X(N+4)^2+W^2)^3)
310  NEXT N
320  Yy(Ii)=Y(Ii)-Yyy
330  Su=Su+Yy(Ii)^2
340  NEXT Ii
350  MAT A=TRN(Aa)
360  MAT B=A*Aa
370  MAT C=A*Yy
380  MAT D=INV(B)
390  MAT Xx=D*C
400  FOR I=1 TO Nn
410  IF ABS(Xx(I))>Aaa THEN 560
420  NEXT I
430  MAT Xxx=X
440  MAT X=Xxx+Xx
450  PRINT X(*);"MAT -X(SOLUTION)"
460  PRINT LIN(2);"TOL=";Aaa,"# OF ITE =";L11,"# OF DATA =";Kk;LIN(3)
470  DISP "RUN WITH NEW DATA ? IF YES THEN PRESS CONT."
480  BEEP
490  PAUSE
500  GOTO 110
510  PRINT "# OF ITER EXCEEDED(";Kkk;")"
```

```
520  DISP "RUN WITH NEW DATA ? IF YES THEN PRESS CONT."
530  BEEP
540  PAUSE
550  GOTO 110
560  MAT Xxx=X
570  MAT X=Xxx+Xx
580  FOR I=1 TO Nn
590  IF X(I)<0 THEN 670
600  IF ABS(X(I))>10^5 THEN 670
610  IF ABS(X(I))<10^(-5) THEN 670
620  NEXT I
630  PRINTER IS 16
640  PRINT "SU=";Su
650    PRINT "ITER #";L11;X(*);"MAT -X"
660  GOTO 190
670  PRINT " NUMBER IS TOO LARGE OR TOO SMALL"
680  PRINT X(*);"MAT-X","LLL=";L11
690  PRINT "RUN AGAIN WITH NEW X0 ?: PRESS CONT."
700  BEEP
710  PAUSE
720  GOTO 110
730  END
```

PLOTING PROGRAM

```
10   OPTION BASE 1
20    DIM X(1000),Y(1000)
30   ! *** SPECIFY MAXIMUM AND MINIMUM VALUE OF DOMAIN AND RANGE
40   INPUT " XMIN = ",Xmin
50   INPUT "XMAX = ",Xmax
60    INPUT " YMIN = ",Ymin
70    INPUT " YMAX = ",Ymax
80    INPUT " DATA INPUT or FUNCTION INPUT (1/-1)",Hhh
81    INPUT "# OF DATA",N
82    REDIM X(N),Y(N)
90    IF Hhh=-1 THEN 190
100   INPUT "# OF DATA ",N
110   REDIM X(N),Y(N)
120   FOR I=1 TO N
130   DISP "X(";I;")";
140   INPUT X(I)
150   DISP "Y(";I;")";
160   INPUT Y(I)
170   NEXT I
180   ! ***  DRAW AXES
190   PLOTTER IS 13,"GRAPHICS"
200   GRAPHICS
210   FRAME
220   PRINTER IS 0
230   RAD
240   LOCATE 10,120,20,90
250   SCALE Xmin,Xmax,Ymin,Ymax
260   Xx=Xmin
270   Yy=Ymin
280   IF Xmin<0 THEN Xx=0
290   IF Ymin<0 THEN Yy=0
300    AXES (Xmax-Xmin)/50,(Ymax-Ymin)/10,Xx,Yy
310   FRAME
320   ! *** LABEL AXES
330   GOSUB Lx
340   GOSUB Ly
350   IF Hhh=1 THEN 770
360   ! *** PLOT
370   A1=885.123
380   A2=693.385
390   A3=935.704
400   A4=856.0189
410   B1=4.099
420   B2=5.205
430   B3=8.6075
440   B4=11.1598
450   C1=18.1728
460   C2=27.62171
470   C3=36.6647
480   C4=46.0456
481   Su=1459.2377
490   PRINT " LORENTZIAN # 1";LIN(2)
500   PRINT "A=";A1,"a=";B1,"H0=";C1;LIN(3)
510   PRINT " LORENTZIAN # 2";LIN(2)
```

```
520  PRINT " A=";A2,"a=";B2,"H0=";C2;LIN(3)
530  PRINT "LORENTZIAN # 3";LIN(2)
540  PRINT "A=";A3,"a=";B3,"H0=";C3;LIN(3)
550  PRINT "LORENTZIAN # 4";LIN(2)
560  PRINT "A=";A4,"a=";B4,"H0=";C4;LIN(3)
561  PRINT "LEAST SQUARES OBJECTIVE FUNCTION =";Su;LIN(3)
570  DEF FNX(X)=4*(A1*B1*(X-C1)/(B1^2+(X-C1)^2)^2+A2*B2*(X-C2)/(B2^2+(X-C2)^2)
2+A3*B3*(X-C3)/(B3^2+(X-C3)^2)^2+A4*B4*(X-C4)/(B4^2+(X-C4)^2)^2)
580  LINE TYPE 3
590  MOVE Xmin,FNX(Xmin)
600  FOR X=Xmin TO Xmax STEP (Xmax-Xmin)/100
610  IF X=0 THEN 630
620  DRAW X,FNX(X)
630  NEXT X
631  LINE TYPE 1
640  ASSIGN #2 TO "DATAE2:T14"
650  READ #2,1;X(*),Y(*)
660  MOVE X(1),Y(1)
670  FOR I=1 TO N
680  DRAW X(I),Y(I)
690  NEXT I
700  ! **** MOVE AND LABEL PLOT
710  MOVE -9,1.1
720  LORG 1
730  CSIZE 5
740 ! LABEL USING " K";" LORENTZ"
750  GOTO 810
760  CSIZE 3
770  MOVE Xmin,Ymin
780  FOR I=1 TO N
790  DRAW X(I),Y(I)
800  NEXT I
810  POINTER -2*PI,.5
820  ! *** ALLOWS YOU TO DIGITIZE
830 Loop: !
840  DIGITIZE X,Y
850  PRINT "X =";X,"Y =";Y
860  GOTO Loop
870  END
880  ! *** LABEL AXES
890 Lx: !
900  CSIZE 3
910  LDIR -(PI/2)
920  LORG 2
930  FOR X1=Xmin TO Xmax STEP (Xmax-Xmin)/10
940  MOVE X1,Ymin
950  LABEL USING " DDZ.DD";X1
960  NEXT X1
970  RETURN
980 Ly: !
990  CSIZE 3
1000 LDIR 0
1010 LORG 8
1020 FOR Y1=Ymin TO Ymax STEP (Ymax-Ymin)/10
```

```
1030 MOVE Xmin,Y1
1040 LABEL USING "DDDDD ";Y1
1050 NEXT Y1
1060 RETURN
```

GAUSS NEWTON WITH 6 VARIATIONS

```
10   OPTION BASE 1
20   DIM Dd(200),Y(200),Yy(200),Aa(200,10),A(10,200),B(10,10),C(10),D(10,10),Xx
10),Xxx(10),X(10),Yw(200),Bw(10,10),Cw(10),Dw(10,10),W1(10,10),W2(10,10)
30   PRINTER IS 16
40    INPUT "# OF VARIABLE",Nn
50   INPUT "TOLERANCE ",Aaa
60   INPUT "# OF ITERATION",Kkk
70   INPUT "# OF INPUT DATA",Kk
80   Sul=100000
90   REDIM Dd(Kk),Y(Kk),Yy(Kk),Aa(Kk,Nn),A(Nn,Kk),B(Nn,Nn),C(Nn),D(Nn,Nn),Xx(Nn)
,Xxx(Nn),X(Nn),Yw(Kk),Bw(Nn,Nn),Cw(Nn),Dw(Nn,Nn),W1(Nn,Nn),W2(Nn,Nn)
100  PRINT USING 190
110  PRINT LIN(3)
120  FOR I=1 TO Kk
130  Dd(I)=I
140  DISP "Y(";I;")";
150  INPUT Y(I)
160  Y(I)=Y(I)+10
170  PRINT USING 180;Dd(I),Y(I)
180  IMAGE 20X,DDD.DDD,5X,DDD.DDD
190  IMAGE 24X,"X",9X,"Y"
200  NEXT I
210   INPUT "CORRECT OR NOT (1/-1)",Nnnn
220   IF Nnnn=-1 THEN 270
230   INPUT "CORRECT VARIABLE # ?",Nnnnn
240   DISP "OLD Y(";Nnnnn;")=";Y(Nnnnn),"NEW Y(";Nnnnn;")";
250   INPUT Y(Nnnnn)
260   GOTO 210
270  Lll=0
280  FOR I=1 TO Nn
290  DISP "X(";I;")";
300  INPUT X(I)
310  NEXT I
320  PRINT X(*);"INITIAL X";LIN(3)
330  INPUT " H0 ?",S
340  DISP "WORKING!!!!!"
350  PRINT "H0=";S
360  Lll=Lll+1
370  IF Lll>Kkk THEN 740
380  Su=0
390  FOR Ii=1 TO Kk
400  H=Dd(Ii)
410  Yyy=0
420  Aa(Ii,6)=0
430  Aa(Ii,1)=0
440  FOR N=2 TO 5
450  W=H-S-(N-2)*X(6)
460  Yyy=Yyy-4*X(1)*X(N)*W/(X(N)^2+W^2)^2
470       Aa(Ii,N)=-4*X(1)*(W/(X(N)^2+W^2)^2-4*W*X(N)^2/(X(N)^2+W^2)^3)
480  Aa(Ii,6)=Aa(Ii,6)-4*X(1)*X(N)*(-(N-2)/(X(N)^2+W^2)^2+4*(N-2)*W^2/(X(N)^2+W^
2)^3)
490  Aa(Ii,1)=Aa(Ii,1)-4*X(N)*W/(X(N)^2+W^2)^2
500  NEXT N
510  Yy(Ii)=Y(Ii)-Yyy
```

```
520  Su=Su+Yy(Ii)^2
530  NEXT Ii
540  PRINT "SUM=";Su
550  IF Su<Sul THEN 570
560  GOTO 950
570  MAT A=TRN(Aa)
580  MAT Yw=Yy
590  MAT B=A*Aa
600  MAT C=A*Yy
610  MAT D=INV(B)
620  MAT Xx=D*C
630  FOR I=1 TO Nn
640  IF ABS(Xx(I))>Aaa THEN 790
650  NEXT I
660  MAT Xxx=X
670  MAT X=Xxx+Xx
680  PRINT X(*);"MAT -X(SOLUTION)"
690  PRINT LIN(2);"TOL=";Aaa,"# OF ITE =";L11,"# OF DATA =";Kk;LIN(3)
700  DISP "RUN WITH NEW DATA ? IF YES THEN PRESS CONT."
710  BEEP
720  PAUSE
730  GOTO 270
740  PRINT "# OF ITER EXCEEDED(";Kkk;")"
750  DISP "RUN WITH NEW DATA ? IF YES THEN PRESS CONT."
760  BEEP
770  PAUSE
780  GOTO 270
790  MAT Xxx=X
800  MAT X=Xxx+Xx
810  FOR I=1 TO Nn
820  IF ABS(X(I))>10^5 THEN 890
830  IF ABS(X(I))<10^(-5) THEN 890
840  NEXT I
850    PRINT "ITER #";L11;X(*);"MAT -X"
860  Sul=Su
870  Mm=0
880  GOTO 360
890  PRINT " NUMBER IS TOO LARGE OR TOO SMALL"
900  PRINT X(*);"MAT-X","LLL=";L11
910  PRINT "RUN AGAIN WITH NEW X0 ?: PRESS CONT."
920  BEEP
930  PAUSE
940  GOTO 270
950  Mm=Mm+1
960  PRINT "MM=";Mm
970  MAT W1=IDN(Nn,Nn)
980  MAT W2=(Mm)*W1
990  MAT Bw=B+W2
1000 MAT Cw=A*Yw
1010 MAT Dw=INV(Bw)
1020 MAT Xx=Dw*Cw
1030 MAT X=Xxx+Xx
1040 PRINT X(*);"MAT-X"
1050 GOTO 360
1060 END
```

GAUSS NEWTON WITH 3 VARIATIONS

```
10   OPTION BASE 1
20   DIM Dd(200),Y(200),Yy(200),Aa(200,10),A(10,200),B(10,10),C(10),D(10,10),Xx(
10),Xxx(10),X(10)
30   PRINTER IS 16
40    INPUT "# OF VARIABLE",Nn
50   INPUT "TOLERANCE ",Aaa
60   INPUT "# OF ITERATION",Kkk
70   INPUT "# OF INPUT DATA",Kk
80   REDIM Dd(Kk),Y(Kk),Yy(Kk),Aa(Kk,Nn),A(Nn,Kk),B(Nn,Nn),C(Nn),D(Nn,Nn),Xx(Nn)
,Xxx(Nn),X(Nn)
90   PRINT USING 170
100  PRINT LIN(3)
110  FOR I=1 TO Kk
120  Dd(I)=I
130  DISP "Y(";I;")";
140  INPUT Y(I)
150  PRINT USING 160;Dd(I),Y(I)
160  IMAGE 20X,DDD.DDD,5X,DDD.DDD
170  IMAGE 24X,"X",9X,"Y"
180  NEXT I
190   INPUT "CORRECT OR NOT (1/-1)",Nnnn
200   IF Nnnn=-1 THEN 250
210   INPUT "CORRECT VARIABLE # ?",Nnnnn
220   DISP "Y(";Nnnnn;")";
230   INPUT Y(Nnnnn)
240   GOTO 190
250  Lll=0
260  FOR I=1 TO Nn
270  DISP "X(";I;")";
280  INPUT X(I)
290  NEXT I
300  PRINTER IS 0
310  PRINT X(*);"INITIAL X";LIN(3)
320  INPUT " H0 ?",S
330 ! INPUT "A ?",Ss
340  DISP "WORKING!!!!!"
350  PRINT "H0=";S
360  Lll=Lll+1
370  IF Lll>Kkk THEN 770
380 ! PRINT "H0 =";S,"A=";Ss
390  Z(2)=1
400  Z(3)=1.59
410  Z(4)=2.33
420  Z(5)=3.16
430  Su=0
440  FOR Ii=1 TO Kk
450  H=Dd(Ii)
460  Yyy=0
470  Aa(Ii,3)=0
480  Aa(Ii,2)=0
490  Aa(Ii,1)=0
500  FOR N=2 TO 5
510  W=H-S-(N-2)*X(3)
```

```
520  Yyy=Yyy-4*X(1)*Z(N)*X(2)*W/(Z(N)^2*X(2)^2+W^2)^2
530        Aa(Ii,2)=Aa(Ii,2)-4*X(1)*Z(N)*(W/(Z(N)^2*X(2)^2+W^2)^2-4*Z(N)^2*W*X(2
^2/(Z(N)^2*X(2)^2+W^2)^3)
540  Aa(Ii,3)=Aa(Ii,3)-4*X(1)*Z(N)*X(2)*(-(N-2)/(Z(N)^2*X(2)^2+W^2)^2+4*(N-2)*W^
2/(Z(N)^2*X(2)^2+W^2)^3)
550  Aa(Ii,1)=Aa(Ii,1)-4*Z(N)*X(2)*W/(Z(N)^2*X(2)^2+W^2)^2
560  NEXT N
570  Yy(Ii)=Y(Ii)-Yyy
580  Su=Su+Yy(Ii)^2
590  NEXT Ii
600  MAT A=TRN(Aa)
610  MAT B=A*Aa
620  MAT C=A*Yy
630  MAT D=INV(B)
640  MAT Xx=D*C
650  FOR I=1 TO Nn
660  IF ABS(Xx(I))>Aaa THEN 830
670  NEXT I
680  MAT Xxx=X
690  MAT X=Xxx+Xx
700  PRINT "LEAST SQUARE SUM=";Su
710  PRINT X(*);"MAT -X(SOLUTION)"
720  PRINT LIN(2);"TOL=";Aaa,"# OF ITE =";L11,"# OF DATA =";Kk;LIN(3)
730  DISP "RUN WITH NEW DATA ? IF YES THEN PRESS CONT."
740  BEEP
750  PAUSE
760  GOTO 250
770  PRINT "# OF ITER EXCEEDED(";Kkk;")"
780  PRINT "LEAST SQUARE SUM=";Su
790  DISP "RUN WITH NEW DATA ? IF YES THEN PRESS CONT."
800  BEEP
810  PAUSE
820  GOTO 250
830  MAT Xxx=X
840  MAT X=Xxx+Xx
850  PRINT X(*);"MAT-X"
860  PRINT "SU=";Su
870  FOR I=1 TO Nn
880  IF ABS(X(I))>10^5 THEN 930
890  IF ABS(X(I))<10^(-5) THEN 930
900  NEXT I
910  ! PRINT "ITER #";L11;X(*);"MAT -X"
920  GOTO 360
930  PRINT " NUMBER IS TOO LARGE OR TOO SMALL"
940  PRINT X(*);"MAT-X","LLL=";L11
950  PRINT "LEAST SQUARE SUM=";Su
960  PRINT "RUN AGAIN WITH NEW X0 ?: PRESS CONT."
970  BEEP
980  PAUSE
990  GOTO 250
1000 END
```

8. REFERENCE

1 L.Kuester and J.H.Mize, "Optimization Techniques With Fortran", p.218-220, Mc Graw-Hill Book Company; New York, 1973.

2 D.E.Kirk, "Optimal Control Theory" ,p.373-394,Printice-Hall Inc, New Jersey, 1970.

3 L.Fisher, J.Mol Spectrosc,40,414-417 (1971).

4 H.A.Jahn and E.Teller Proc.Roy.Soc A(161) (1937)220.

5 F.S.Ham,Jahn-Teller Effects in Electron Paramagnetic Resonance Spectra, Plenum Publishing Company, New York. 1968.

6 M.C.M O' Brien Proc.Roy.Soc.A(281) (1964)232.

7 D.P.Breen,D.C.Krupka and F.I.B. Williams, Phys.Rev.179(1969) 241.

8 A.Abragam and B.Bleaney, "Electron Paramagnetic Resonance of Transition Ions", p.454-466, Clarendon Press, Oxford,1970.

9 L.S. Dang, "ETUDE DES PHENOMENES DYNAMIQUES DANS UN SYSTEME. JAHN -TELLER CAS PARTICULIER DE L' ION Cu^{2+} DANS $ZnSi\ F_6,6H_2O$: unpublished thesis, University of Grenoble, 1972.

10 D.P. Breen,D.C.Krupka and F.I.B.Williams,Phys.Rev.vol.179,No 2, 255-272, 1969.

11 C.P.Slichter, "Principles of Magnetic Resonance",Frederick Seitz, Harper &Row Publishs,New York, 1963.

12 G.E.Pake, "Paramagnetic Resonance", W.A. Benjamin Inc., New York, 1962.

13 C.Kittel, "Introduction to Solid State Physics", Willey Eastern Private Limited, New Delhi, Chapter 16, p.535-634, 1968.

14 D.P Breen and L.S. Dang, "Investigation into the variable with temperature in the EPR spectrum of Jahn-Teller system",'Symposium of Physics', Singapore, 1972, p.84-95.

15 R.E.Miller, "Modern Math Methods for Economics and Business", Holt Rinehart&Winstan, New York, 1972.